Projecting Future Climate Change: Implications of Carbon Cycle Model Intercomparisons

Haroon S. Kheshgi

Corporate Strategic Research, ExxonMobil Research and Engineering Company

Annandale, NJ 08801, U.S.A.

Atul K. Jain

Department of Atmospheric Sciences**,** University of Illinois

Urbana, IL 61801, U.S.A.

Abstract

Models simulate responses of future climate to scenarios for anthropogenic emissions. While the uncertainty of these simulated responses is not established, perspective on uncertainty is provided by the intercomparison of the responses of alternative models. The envelope of alternative model simulations, if plausible responses, must be contained within the uncertainty range. In this way model intercomparisons form a lower-bound estimate of uncertainty range of future response. In this study, a parameterized Earth system model is used as a meta-model to simulate responses of alternative detailed models for the ocean and biosphere components of the global carbon cycle. The meta-model allows the integration of these components of the carbon cycle with an energy balance climate model for a prescribed range of climate sensitivity. The meta-model, parameterized in this way, is then used to construct ranges of: 1) past carbon budgets given past CO_2 concentrations, fossil carbon emissions, and temperature records, 2) future CO_2 concentrations and temperature for given emission scenarios, and 3) CO_2 emissions and temperature for given trajectories of future CO_2 concentrations leading to constant levels within the next several centuries. Uncertainty in projections of future CO_2 concentration contributes to the range of future global temperature projected in this way. Carbon cycle is an additional contributor to uncertainty in climate projections that further expands the range of climate projections beyond that assessed by the Intergovernmental Panel on Climate Change.

1. Introduction

Global carbon cycle is one link in a causal chain linking human activities to changes in climate. The causal chain includes relations between human activities, emissions of greenhouse gas concentrations, alteration of components of the climate system (greenhouse gas concentration, aerosols, land cover, etc.), changes in the radiative balance of the atmosphere, and the response of climate. The behavior of global carbon cycle determines the response of the atmospheric concentration of CO_2, the greenhouse gas of greatest concern, to sources and sinks of CO_2 from a wide range of human activities, particularly CO_2 emissions from fossil fuel consumption. Currently, our ability to forecast future climate is in question. Models are used to make projections of future climate, based on scenarios of future human activities and emissions, by simulating each link in the causal chain relating these scenarios to changes in climate. The estimation of the uncertainty of this causal chain remains an important scientific challenge.

Global carbon cycle, the link relating emissions of CO_2 to its concentration is often *assumed* to lead to relatively certain predictions of its behavior given the clear trend in the concentration of CO_2 and the clear attribution of the anthropogenic cause of this trend. Climate projections [*Cubasch et al.,* 2001] communicated by the Intergovernmental Panel on Climate Change (IPCC) in its Third Assessment Report (TAR) did not account for uncertainty in future carbon cycle behavior. Uncertainty in carbon cycle behavior was, however, assessed in the reported IPCC CO_2 projections [*Prentice et al.,* 2001], and carbon cycle model intercomparison was one approach used to make this assessment -- details of this approach are later given in this paper. A wide

range of behavior of global carbon cycle is exhibited by current detailed carbon cycle models resulting in a wide range of projected CO_2 concentration, given a scenario for emissions; this range is wider than had been considered in previous assessments and contrary to the common assumption. Consequently, when accounted for in simulation of the entire climate system, the range of climate projections also becomes wider.

Many types of models are used to simulate carbon cycle on different spatial and temporal scales. For the assessment of the effects of anthropogenic emissions on climate, the global scale is of interest and time scales spanning decades to centuries are relevant. Methods are needed to characterize the uncertainty of such projections under these conditions, even though the result may be ambiguous. A challenge for global carbon cycle models is to forecast the response of ocean, plant and soil carbon uptake under conditions unprecedented in history. The limited opportunities to validate such models by comparison to data, therefore, only arise under conditions or scales different than an assessment model's task.

Approaches that have been used to provide information about the uncertainty of projections have included model sensitivity analysis, model calibration, and model intercomparison. Model sensitivity can be used to assess uncertainty if the model structure is accurate and if there is sufficient information about model parameters. For example, Joos et al. [2001] made bounding assumptions on the ranges of some parameters of their climate/carbon system model to produce a bounding range of CO_2 concentration projections, one approach used in the IPCC TAR [*Prentice et al.,* 2001]. Model calibration can be used to estimate model parameters provided the model structure is correct and data is available with which to calibrate the model. In the IPCC Special

Report on Radiative Forcing (SRRF) [*Schimel et al.*, 1995] and the Second Assessment Report (SAR) [*Schimel et al.*, 1996], ocean tracer data along with model intercomparisons were used to calibrate global carbon cycle models to give bounds on CO_2 projections. Of course, the best of both approaches can be combined by Bayesian parameter estimation applying prior information about model parameters as well as observation-based constraints [c.f. *Kheshgi et al.*, 1999; *Kheshgi and Jain*, 2000]. Parameter estimation, however, may not give reliable results if the correct model structure is not known. Model intercomparisons can provide some information about plausible model structures as well as providing information about the uncertainty of projections. The envelope of alternative model simulations, if plausible responses, must be contained within the uncertainty range. In this way model intercomparisons form a lower bound on the estimated uncertainty range of future response. However, guidelines for model intercomparisons often restrict the possible responses, leading to an underestimate of the lower bound. Guidelines may include, for example, specification of future climate or over-calibration to past response [c.f. *Enting et al.*, 1994]. Model calibration, or model sensitivity, has in many cases been applied to a restricted set of model parameters without full consideration of the uncertainty of observations or model limitations. In this study we begin to address these deficiencies, and make new reconstructions of past carbon budgets, projections of CO_2 concentration and temperature for given scenarios of future emissions, and estimate implications of concentration stabilization on CO_2 emissions and temperature. The range of CO_2 projections detailed

here were also used in the IPCC TAR [*Prentice et al.*, 2001], however, the climate projections were not.

Increasing levels of detail are being required to simulate mechanisms hypothesized to be important for global carbon cycle, and to allow comparison to observational data on the scales on which the data are available. More specifically, there are apparent relations between, for example, climate and carbon cycle; hypothesized mechanisms that might be responsible for these relations require spatial and temporal resolution to simulate to compare to data [e.g. *Heimann et al.*, 1998; *Le Quéré et al.*, 2000]. In this study we use a globally aggregated climate/carbon cycle model as a meta-model to represent the globally aggregated responses of detailed models for the ocean and terrestrial biosphere components of the Earth system that have been catalogued in model intercomparison studies [*Cramer et al.*, 2001; *Orr et al.*, 2001; *Prentice et al.*, 2001]. In section 2, the meta-model is described along with its calibration to results of model intercomparisons. In section 3, the past response of global carbon cycle is reconstructed using this meta-model. This reconstruction includes past carbon budgets that are compared to budgets based on observational constraints. In addition, specification of observed past climate introduces an adjustment of the carbon budgets based on carbon cycle models over the past decades not included in past assessments. In section 4, future projections of CO_2 and global temperature are made driven by emission scenarios, and including the range of meta-model parameters calibrated to reproduce model intercomparison results. Ranges of CO_2 projections presented here, and in the IPCC TAR, are wider than presented in past IPCC assessments. And ranges of projected

global mean temperatures presented here are wider than presented in the IPCC TAR in which uncertainty in CO_2 concentration was not included in ranges of climate projections. Finally, projections beyond a century in duration leading to constant levels of CO_2 concentration show the increasing importance -- with time in this model simulation -- of the ocean carbon sink relative to that of the terrestrial biosphere.

2. Methodology

2.1. Use of ISAM as a Meta-Model for the Carbon/Climate System

The Earth system exhibits interactions between carbon cycle and climate, as well as effects of human activities through land use and other alterations of the environment. Climate can be affected by carbon cycle through two pathways: change in CO_2 concentration (through its greenhouse effect), and change land cover (through, e.g., albedo and evapotranspiration). Climate affects the growth, disturbance and respiration of plants and soils, the terrestrial component of global carbon cycle relevant over time scales from years to centuries. Climate also affects the oceans' role in global carbon cycle through the effect of temperature on the relation between total dissolved carbon and the partial pressure of CO_2 , and through potential climate-induced changes in ocean transport and biological activity. The ocean and terrestrial components of carbon cycle

are connected through the atmosphere, and to a lesser extent through runoff of terrestrial carbon to the oceans.

A variety of detailed models for climate and components of the carbon cycle have been developed. In addition, detailed models are being coupled to approximate the Earth system in increasing detail, but only for select detailed component models. To approximate the behavior of combinations of many detailed component models, a globally aggregated (i.e. reduced form) Earth system model, the Integrated Science Assessment Model, ISAM [*Jain et al.*, 1994; *Jain and Hayhoe*, 2001], is used in this study as a meta-model.

The global carbon cycle component of ISAM depicted in Fig. 1 is used to simulate the exchange of carbon dioxide between the atmosphere, reservoirs of carbon in the terrestrial biosphere, and the ocean column and mixed layer [*Jain et al.*, 1994; *Jain et al.*, 1995; *Jain et al.*, 1996; *Kheshgi et al.*, 1996; *Kheshgi et al.*, 1999]. The model consists of a homogeneous atmosphere, an ocean mixed layer and land biosphere boxes, and a vertically-resolved upwelling-diffusion deep ocean. The detailed description of the ocean and land-biosphere components of this model are given by Jain *et al.* [1995], and Kheshgi *et al.* [1996], respectively, and a discussion of model parameters by Kheshgi *et al.* [1999]. In this model, the thermohaline circulation is schematically represented by polar bottom-water formation, with the return flow upwelling through the 1-D water

column to the surface ocean from where it is returned, through the polar sea, as bottom water to the bottom of the ocean column thereby completing the thermohaline circulation. The response of bottom-water carbon concentration to changes in the mixed-layer concentration is modeled parametrically by the parameter π_c as described in detail by Jain *et al.* [1995]. A marine biosphere source term is included in the deep sea associated with the oxidation of the organic debris exported from the mixed layer where it is produced by photosynthesis [*Volk and Hoffert,* 1985; *Jain et al.,* 1995].

To estimate terrestrial biospheric fluxes, a six-box globally aggregated terrestrial biosphere submodel is coupled to the atmosphere box (Fig. 1). The terrestrial biosphere model is made up of six boxes which represent ground vegetation, non-woody tree parts, woody tree parts, detritus, mobile soil with a turnover time 70 years, and resistant soil with a turnover time 500 years. The mass of carbon contained in the different reservoirs and their turnover times as well as the rates of exchange between them have been based on the analysis by Harvey [1989a] and Kheshgi *et al.* [1996]. The effects of land use are included by changing (decreasing with time) the total productive land area covered by the terrestrial biosphere. The carbon mass in each of the boxes is proportional to the total productive land area. Decreases in area lead to CO_2 emissions due to changes in land use as well as a decrease in the global rate of carbon exchange with the (smaller) biosphere. A simple model representation of biospheric response to changes in the atmospheric

concentration of CO_2 and the global mean-annual near-surface temperature over land are included. An increase in the rate of net photosynthesis of trees or net primary productivity of ground vegetation, relative to pre-industrial times, is modeled to be proportional to the logarithm of the relative increase in atmospheric CO_2 concentration from its pre-industrial value. The magnitude of the modeled biospheric sink depends primarily on the chosen value of the proportionality constant ß, the CO_2 fertilization factor [*Keeling*, 1973; *Harvey*, 1989b; *Wigley*, 1993]. Exchange of carbon to and from terrestrial biosphere boxes (respiration, translocation and photosynthesis) vary with global mean annual temperature according to a Q_{10} formulation, i.e. where net primary production, translocation, and respiration rates are proportional to $\left(Q_{10}\right)^{T/10^{\circ}C}$: where T is the global-mean land temperature and Q_{10} is a model parameter [*Harvey*, 1989a].

In the reduced form model ISAM, the carbon cycle components are coupled to each other through the atmosphere, and to a reduced-form energy-balance climate model of the type used in the 1990 IPCC assessment [*Hoffert et al.*, 1980; *Bretherton et al.*, 1990]. Carbon cycle's influence on global temperature due to the greenhouse effect of CO_2 is accounted for, although that due to change in land cover is neglected. And global temperature is modeled to influence carbon cycle leading to a *climate feedback* on carbon cycle. In the IPCC SAR, projections of atmospheric CO_2 using ISAM were included, although the climate feedback was turned off [*Schimel et al.*, 1996; *Harvey et al.*, 1997].

To use ISAM as a meta-model, the terrestrial and ocean carbon cycle components of ISAM are callibrated to match the range of behavior of results of model intercomparisons of detailed terrestrial and ocean component models: see Sections 2.2.1 and 2.2.2, respectively. A range of climate model parameters are specified: see Section 2.2.3. The range of intergrated system response is calculated by running ISAM with the ranges of parameters determined in this way. Results are presented for past carbon cycle in Section 4, and for future scenarios in Section 5.

2.2. Meta-Model Calibrations

2.2.1 Terrestrial Carbon Cycle

The terrestrial (plants, litter and soils) component of ISAM is calibrated to reproduce the net terrestrial uptake over a decade to century time scale of six dynamic global vegetation models (DGVMs) that have been intercompared for a common scenario of CO_2 and climate.

The DGVM intercomparison summarized by Cramer et al. [2001] reports the results of six DGVMs: HYBRID [*Friend et al.*, 1997], IBIS [*Foley et al.*, 1996], LPJ [*Sitch*, 2000], SDGVM [*Woodward et al.*, 1998], TRIFFID [*Huntingford et al.*, 2000], and VECODE [*Brovkin et al.*, 1997]. Each model simulates linked changes in ecosystem function (water, energy and carbon exchange) and vegetation structure (distribution,

physiognomy) in response to a common scenario of changes in CO_2 concentration and climate. The CO_2 concentration scenario, shown in Fig. 2, was associated with IPCC emission scenario IS92a [*Leggett et al.*, 1992] -- c.f. the analysis of IS92a from this study in Section 4.1. This same CO_2 scenario was used as input for the coupled atmosphere-ocean general circulation model HadCM2-SUL [*Mitchell et al.*, 1995] that is a simulation of the climate response to the IPCC emission scenario IS92a. This climate simulation was the climate scenario used in this intercomparison with some modification [see *Cramer et al.*, 2001]. The annual global land temperature of this modified scenario is shown in Fig. 2.

The results of the DGVMs show considerable variability in the terrestrial uptake of carbon in addition to their response to changing CO_2 and climate. Fig. 3 shows a running ten-year mean of annual global uptake for the DGVM results corresponding to the common scenario for changing CO_2 and climate. Variations in the ten-year budget of carbon uptake is of similar magnitude to the mean uptake over the past two decades for some models. Year-to-year variations are larger. Over the period from 2000 to 2050, all models show significant carbon uptake in response to the scenario. Beyond 2050, all models except for the HYBRID model exhibit continued uptake.

The globally aggregated terrestrial component of ISAM used in this study is driven by changes in atmospheric CO_2, temperature and land use. Since results from Cramer et al. [2001] do not include land use, the absence of land use (pre-anthropogenic conditions) is specified in ISAM for comparison to DGVM results. Since the future cumulative change in carbon stocks in the terrestrial biosphere is more closely related to

change in future atmospheric CO_2 concentration over the next century than annual uptake, ISAM is calibrated to match this feature of the DGVM results shown in Fig. 4.

In the first step of the ISAM calibration, the strength of the modeled CO_2 fertilization effect, represented by model parameter *ß*, is adjusted to match DGVM results driven by changes in atmospheric CO_2 concentration with no change in climate. As a *reference* case, the results of ISAM matching the average of the results of the IBIS, LPJ and SDGVM models corresponds to *ß* = 0.52. A stronger terrestrial sink would correspond to a larger value of *ß* and a *lower* projection of future CO_2. To define a range of model responses, model parameters corresponding to *low* and *high* projections of CO_2 are estimated. The range of DGVM responses are spanned by ISAM results with *ß* = 0.35 (*high* parameterization) to 0.9 (*low* parameterization): see Fig. 4a. Note that the value of *ß* used in ISAM projections for the IPCC SAR was 0.39 [*Jain et al.*, 1996], at the low end of this range; however, the results used in the SAR did not include the feedback of climate on carbon cycle.

In the second step of the ISAM calibration, the strength of the modeled temperature effects on productivity of non-woody tree parts and the translocation from non-woody to woody tree parts, represented by model parameters $Q_{10,\,np}$ and $Q_{10,\,t}$, are adjusted to match DGVM results driven by changes in both atmospheric CO_2 concentration and climate. The Q_{10} coefficients for temperature sensitivity of respiration and exchange between other soil and plant reservoirs remain unchanged from their values used in prior studies [*Harvey*, 1989a; *Kheshgi et al.*, 1996]. We choose to adjust the Q_{10} coefficients related to net primary productivity (NPP) because the sensitivity of NPP of DGVMs to increases in temperature differs drastically (even in sign) between DGVMs [*Cramer et al.*, 1999]. We note that DGVMs respond to aspects of climate (e.g. precipitation and cloudiness) in addition to annual global land temperature. The only

climate input to ISAM is annual global land temperature, taken as an anomaly from the 1861 to 1900 average land temperature shown in Fig. 2. Calibration of the ISAM model to match DGVM results implicitly includes the effects of these other aspects of climate; how good this implicit approximation is could be tested by comparing to DGVM results driven by other climate scenarios, however, these are not available. In addition, other potential drivers such as nitrogen deposition and changes in ozone levels are neglected in both the DGVM and ISAM results. These additional effects may contribute to the uncertainty in projections.

Again a reference, low and high ISAM parameterization is estimated to reproduce the carbon accumulation response of the DGVMs over the time period from 2000 to 2100: see Fig. 4b. For the reference, low and high parameterizations the Q_{10} coefficient for net productivity of the non-woody carbon reservoir (see Fig. 1) is 1., 0.75 and 1.2, respectively -- all are lower than in prior studies [*Harvey*, 1989a; *Kheshgi et al.*, 1996]. For all three parameterizations the Q_{10} coefficient for translocation from the non-woody to woody reservoirs is reduced to 1.2 from that in prior studies to avoid an excessive build-up in the non-woody reservoir. While productivity in these parameterizations of ISAM all increase with increasing temperature, productivity does not increase as much as does respiration. The net result is less terrestrial carbon accumulation compared to the results (Fig. 4a) without climate change. Note that the low parameterization has both a stronger modeled CO_2 fertilization effect and a weaker temperature productivity sensitivity than the reference case. The high parameterization has the opposite. The effect of increasing temperature, therefore, decreases the width of the range of modeled terrestrial carbon accumulation from that without climate change.

2.2.2 Ocean Carbon Cycle

The ocean component of ISAM is calibrated to reproduce the net ocean uptake over a decade to century time scale of ten detailed ocean carbon cycle models that have been intercompared for the common scenario of CO_2 given in Fig. 2.

The ocean model intercomparison organized under the Ocean Model Intercomparison Project -- OCMIP -- [*Orr and Dutay*, 1999] provided the results [*Prentice et al.*, 2001] of ten detailed ocean carbon cycle models labeled with the acronyms: 1) AWI -- Alfred Wegener Institute for Polar and Marine Research, Bremerhaven, Germany; 2) CSIRO, Hobart, Australia; 3) IGCR -- IGCR/CCSR, Tokyo, Japan; 4) IPSL -- Institute Pierre Simon LaPlace, Paris, France; 5) LLNL, Livermore, California, USA; 6) MPIM -- Max Planck Institut fuer Meteorologie, Hamburg, Germany; 7) NCAR -- National Center for Atmospheric Research), Boulder, Colorado, USA; 8) PIUB -- Physics Institute, University of Bern, Switzerland; 9) PRINCE -- Princeton University (AOS, OTL) / GFDL, Princeton NJ, USA; 10) SOC -- Southampton Oceanography Centre / SUDO / Hadley Center, UK Met. Office, England.

The ocean CO_2 uptake response of the OCMIP models to changing atmospheric CO_2 concentration is shown in Fig. 5. All of the responses show an increasing uptake of carbon. Variability in annual uptake is small in comparison to the magnitude of uptake, unlike the results of DGVMs. Acumulation of carbon in the oceans from 2000 to 2100 (Fig. 5b) is of comparable magnitude to that of the modeled terrestrial biosphere (Fig. 4).

The response of the globally aggregated ocean component of ISAM used in this study to in atmospheric CO_2 depends on ocean transport parameters: effective vertical diffusivity, upwelling velocity, and the change in bottom-water concentration relative to the change in mixed layer concentration is modeled parametrically by the parameter π_c. The latter parameter is poorly constrained by ocean tracers and has a large effect on the ocean carbon budget over a decade to century time-scale [*Kheshgi et al.*, 1999]. ISAM is calibrated to match the average and range of all ten OCMIP responses by adjustment of parameter π_c leaving remaining ocean parameters at the values used in prior studies [*Jain et al.*, 1995; *Kheshgi et al.*, 1999]. The average response of the OCMIP models is matched using $\pi_c = 0.475$, and the range is spanned with $\pi_c = 0.807$ (low parameterization) to $\pi_c = 0.072$ (high parameterization) compared with $\pi_c = 0.5$ used in prior studies [*Jain et al.*, 1995; *Schimel et al.*, 1995; *Schimel et al.*, 1996]. Comparison between the annual and cumulative uptake of the ISAM calibrated in this way is compared to that of the ten OCMIP models in Fig. 5.

As noted by Prentice et al. [2001] and references therein, the effects of temperature on total dissolved carbon solubility dominate the modeled climate's effect on ocean uptake for scenarios such as this one prior to 2050. After that time, changes in ocean stratification begin slow ocean uptake further in coupled ocean carbon cycle/climate simulations. The comparison to OCMIP results presented here did not include effects of changing climate. ISAM does include effects of ocean surface

temperature on total dissolved carbon solubility -- we expect that the ISAM aggregated model for this effect will accurately reproduce this effect as seen in detailed models [c.f. *Joos et al.*, 1996; *Kheshgi and White*, 1996]. ISAM does not, however, include effects of climate on ocean stratification.

2.2.3 Climate/Carbon System

In ISAM, a reduced-form energy-balance climate model of the type used in the 1990 IPCC assessment [*Hoffert et al.*, 1980; *Bretherton et al.*, 1990] is used to calculate global mean-annual near-surface temperature. In this energy balance model, radiative forcing of climate is balanced by accumulation of heat in the oceans and enhanced outgoing (infrared) radiation due to increased global temperature.

Radiative forcing of climate is calculated from the same relations between greenhouse gas concentrations and aerosols as was used in the IPCC TAR [*Ramaswamy et al.*, 2001]. Notably, the radiative forcing for a doubling of CO_2 concentration is ΔF_{2x} = 3.7 Wm^{-2} [*Ramaswamy et al.*, 2001], a 15% lower radiative forcing compared with the value of 4.37 Wm^{-2} used in previous assessments [*Harvey et al.*, 1997].

A key factors relating radiative forcing change to global temperature change in the ISAM model is the equilibrium climate sensitivity for a doubling of CO_2 concentration, ΔT_{2x}. Equilibrium climate sensitivity is one factor used to account for the

uncertainty in future global climate projections even though a full characterization of uncertainty of climate projections is not well characterized [e.g., *Morgan and Keith*, 1995]. We use a reference value of climate sensitivity of 2.5°C for a radiative forcing increase produced by a doubling of CO_2, and test the sensitivity to this parameter over the range of climate sensitivity from 1.5°C to 4.5°C, the range still considered to be appropriate by the IPCC [*Cubasch et al.*, 2001]. Since higher temperature is associated with less uptake of CO_2 by the ocean and biosphere in the model intercomparisons above, we associate a climate sensitivity of 4.5°C with our high CO_2 parameterization of ISAM and 1.5°C with our low parameterization. Note that retaining the same ΔT_{2x} while reducing the estimate of ΔF_{2x} by 15% implies that the climate sensitivity parameter $\lambda \equiv \Delta T_{2x}/\Delta F_{2x}$ is implicitly revised upward 15%.

In ISAM, ocean heat transport follows the same transport scheme and parameters as does transport of dissolved inorganic carbon. Therefore, for the reference and range of projections calculated in the following section, the ocean parameters found to fit the ocean carbon cycle results in Section 2.3 are used as well for ocean heat transport.

Global temperature change projected by the model is used as an index of climate change, as is land temperature change is in Section 2.2. Coupled ocean/atmosphere general circulation models appear to all exhibit greater warming over land than over the oceans when forced with increasing greenhouse gas concentrations [*Cubasch et al.*,

2001]. To approximate this effect, the land temperature anomaly (from the pre-anthropogenic model equilibrium) is taken to be 25% larger than the global temperature change calculated by the ISAM energy balance model. This land temperature change is used as input into the terrestrial carbon cycle component of ISAM for both projections of future climate change using ISAM projections of global temperature anomaly, as well as past reconstructions using observation-based estimates of global temperature anomaly.

There are other factors influencing climate (solar fluctuations, volcanoes, ocean current variations) that result in climate variability that is not represented in ISAM projections. In addition, there is considerable uncertainty in the radiative forcing of climate from, e.g., aerosols [*Schwartz and Andreae*, 1996], that are not considered in this study. Furthermore, this study uses global mean-annual temperature anomaly as a proxy for climate change that affects global carbon cycle. Regional patterns and precipitation will have some affect on carbon storage in plants and soils that remains to be better understood before incorporation into a meta-model study such as this one introducing a additional source of uncertainty not included in this study, which forms a lower bound on the estimated uncertainty range of future carbon cycle response.

3. Reconstruction of Past Carbon Cycle

The ISAM model is used to reconstruct the past globally aggregated response of carbon cycle to observed changes in atmospheric CO_2, temperature and estimated fossil fuel emissions for the three different model parameterizations. ISAM reconstructions start from a steady state model solution with temperature anomaly equal to zero and atmospheric CO_2 of 278 ppm. The model solutions span from 1765 through 1999.

Figure 6 shows the atmospheric CO_2 and temperature inputs for ISAM over the period from 1765 through 1999. Estimates of atmospheric CO_2 concentration from ice cores and direct measurements given by Enting et al. [1994] are specified from 1765 through 1972. The average of annual concentrations from the Mauna Loa (Hawaii) and South Pole Observatories [*Keeling and Whorf*, 2000] is specified for the period from 1973 through 1999. The annual globally aggregated near-surface temperature estimated by Jones et al. [2000] is specified from 1856 through 1999 as an anomaly from its average from 1856 through 1875 (for prior times, 1765 through 1855, it is set to zero). Estimates of global annual emissions from fossil fuel burning and cement production made by Marland et al. [2000] are specified from 1765 through 1997. Emissions for 1998 and 1999 are estimated by applying emissions factors [*IPCC*, 1997] to energy consumption statistics [*British Petroleum Company*, 2000] to calculate emissions over the period from 1997 though 1999. This emission estimate is then scaled to match the Marland et al. [2000] estimates for emissions from fossil fuel burning and cement production in 1997. The resulting emission estimate for 1998 and 1999, therefore, implicitly includes emissions from cement production.

The modeled uptake of CO_2 by the oceans is calculated in response to the specified changes in atmospheric CO_2 and temperature. However, to calculate the net terrestrial (i.e. from plants and soils) source or sink of CO_2 from the terrestrial carbon cycle model requires the additional specification of a history of land use emissions, and estimates of past land use emissions remain very uncertain. To balance the carbon budget, emissions of fossil carbon must equal accumulation of carbon in the atmosphere, ocean and terrestrial reservoirs. This constraint provides an alternative means to deduce the net terrestrial source of carbon. The land use emission is then deduced to be that required for the model to match this net terrestrial source. The difference between the net terrestrial source and the deduced land use emission is therefore the modeled terrestrial response to changes in atmospheric CO_2 and temperature. The terrestrial response, however, does depend on the history of land use in ISAM, and so a sequential iterative method is used to converge on this match [*Kheshgi et al.*, 1996]. Land use emissions deduced in this way can be compared to independent emission estimates as one test for model consistency.

Model-based reconstruction of carbon budgets over different time periods for the three model parameterizations are given in Table 1. Since fossil CO_2 emissions and atmospheric CO_2 concentration are model inputs independent of model parameterization, the budget quantities for these are common for the three parameterizations.

Modeled ocean uptake is driven by changes in CO_2 and temperature. Temperature rise is particularly strong in the Jones et al. [2000] temperature record, Figure 6, over the past two decades. Over periods of rising temperature, modeled ocean uptake is lower than if temperature did not change. This causes modeled ocean uptake

over the 1980s and 1990s to be lower by about 3 GtC (0.3 GtC/yr) over each decade in Table 1, than in the ocean model intercomparison without climate change. Note that in this reconstruction, we impose an average surface temperature change matching the global temperature record; the modeled ocean heat content responds to the surface temperature change. If, however, temperature change were driven by changes in ocean circulation, then the relation between surface temperature and ocean CO_2 uptake could be the opposite than is modeled. This is what may happen, for instance, in temperature variations caused by ENSO events [*Archer et al.*, 1996; *Feely et al.*, 1999]. While changes in ocean heat transfer might cause its effect on ocean CO_2 uptake to have varied over the past, the accumulation of total ocean heat apparent in ocean temperature records [*Levitus et al.*, 2000] implies that over the past century the oceans have warmed along with the surface temperature in accord with the modeled mechanism.

Early IPCC assessments of carbon budgets [*Schimel et al.*, 1995], the ocean sink of carbon in the 1980s was estimated to be 20 ± 8 Gt C (90% confidence interval) based primarily on ocean carbon cycle models calibrated with bomb-radiocarbon constraints. Extending these models to the 1990s gave an estimate of 23 ± 8 Gt C [*Bolin et al.*, 2000]. Inclusion of both ^{13}C and ^{14}C constraints, along with modeled temperature change, led to a slightly lower estimate of 17 ± 7 Gt C (90% confidence interval) for the 1980s [*Kheshgi et al.*, 1999]. O_2/N_2 data available for the 1990s has led to a nearly model independent estimate of 17 ± 8 Gt C (90% confidence interval) for the 1990s [*Prentice et al.*, 2001], although this estimate is sensitive to various corrections for temperature change [*Le Quéré et al.*, 2001]. In addition, the net ocean uptake of CO_2 due to the entire anthropothropogenic perturbation of carbon cycle has been estimated indirectly using

oceanic observations [*Gruber et al.,* 1996]; for the period up until 1990, a global estimate of 107 ± 27 Gt C [one standard error, see *Prentice et al.,* 2001] has been made which compares well with the reference case value of 106.6 Gt C (Table 1). The ISAM range of ocean uptakes for these decades listed in Table 1 are within all of these uncertainty ranges and spans a narrower range.

In past IPCC assessments of carbon budgets, the net terrestrial sink was deduced from the budget given an estimate of fossil fuel emissions, atmospheric emissions and ocean uptake [*Watson et al.,* 1990; *Schimel et al.,* 1995; *Schimel et al.,* 1996; *Bolin et al.,* 2000; *Prentice et al.,* 2001]. And in IPCC assessments, the residual terrestrial sink was then deduced from the budget provided an estimate of land use emissions is available. The residual terrestrial sink could then be compared to estimates of sinks due to different factors: CO_2 and nitrogen fertilization and climate change [*Schimel et al.,* 1995].

In this model reconstruction of the past carbon budget, ranges of net terrestrial uptake, based on ranges of ocean model uptake, are calculated from budgets in Table 1. Unlike the IPCC budgets, however, ranges of land use emissions are deduced, based on ranges of terrestrial model responses (to temperature and CO_2) listed in Table 1. Land use emissions deduced in this way can be compared to estimates of land use emissions.

Independent (of the global carbon budget) estimates of land use emissions are, for example, 17 ± 8 Gt C [*Bolin et al.,* 2000; *Houghton,* 2000] for the decade of the 1980s, and 16 ± 8 Gt C [*Bolin et al.,* 2000] for the 1990s. The ranges of budget-deduced land use emissions in Table 1, however, extend to much lower values, especially in the 1990s. Estimates of land use emissions may well form a constraint on this range of model results. However, there potentially is considerable variability in terrestrial carbon uptake over a decade, as is evident in the responses of the DGVMs in Figure 3. Furthermore, the

decade time-scale variability in DGVM uptake is not similar between all DGVMs and is not reproduced, or intended to be reproduced, by the ISAM model. This limits the direct application of the land use emission estimates for a single decade as a constraint on the range of century time-scale terrestrial model response as has been done in past IPCC assessments [*Schimel et al.*, 1995; *Schimel et al.*, 1996]. Observed terrestrial carbon uptake over a single decade will be of limited use to calibrate terrestrial carbon cycle models until variability in terrestrial uptake is understood. Consideration of longer budget periods (c.f. Table 1) may mute this effect of variability of terrestrial CO_2 uptake. Changes in land uses have led to an estimated net emission of CO_2 of 121 Gt C from 1850 to 1990 [*Houghton*, 1999; *Houghton*, 2000], as well as an estimated 60 Gt C prior to 1850 [*DeFries et al.*, 1999]. These estimates are well within the range of model budget deduced land use emissions in Table 1.

4. Projections of Future Carbon Cycle

4.1. IS92a Benchmark Scenario

Model-based estimates of the global carbon budget and climate effects are extended into the future by specification of scenarios of CO_2 emissions from fossil fuels and land use, as well as the emission of other greenhouse gases, aerosols and aerosol precursors. In this section, the IPCC emission scenario IS92a [*Leggett et al.*, 1992] is used as a benchmark to compare coupled model projections to those given in other studies: fossil CO_2 emissions for this scenario are shown in Fig. 7a.

To initiate ISAM projections, observation-based estimates of atmospheric CO_2 concentration, fossil emissions, and global temperature anomaly are used though 1999, as described in Section 3. From the year 2000 through 2100, projections are made with the three parameterizations of ISAM including the range of climate sensitivities discussed in Section 2.4. The carbon budgets for these projections from 2000 through 2099 is summarized in Table 2, CO_2 concentrations are given in Fig. 7b, and projected global temperature anomalies in Fig. 7c. A single estimate of radiative forcing (as a function of time) from other greenhouse gases and aerosols is input over this time period consistent with that given in the IPCC TAR [*Ramaswamy et al.*, 2001], therefore, the sensitivity to uncertainties in these contributors to radiative forcing are not included. ISAM projections for the IS92a scenario in 2100 for the reference (low, high) parameterization for CO_2 concentration is 723 (640 - 804) ppm. As is evident in the carbon budget in Table 2, the range in accumulation of plant and soil carbon stocks is the primary source of width of range in atmospheric CO_2 concentration projections. Projected global temperature anomaly in 2100 is 2.9 (1.7 - 5.6) ^{o}C (recall that this is the anomaly from the pre-anthoropogenic model equilibrium). The difference between the projected global temperature anomaly in 2100 and the observation-based anomaly in 1990 -- taken to be 0.68 ^{o}C -- is, therefore, 2.2 (1.0 - 4.9) ^{o}C. The range in climate sensitivity and CO_2 concentration are both primary contributors to the range in projected temperature in 2100. Results of this benchmark scenario can be compared to other studies.

The IPCC SRRF (Schimel et al. 1995) presented the results of an intercomparison of 18 global carbon cycle models [*Enting et al.*, 1994]. The terrestrial carbon cycle components of these models did not include the range of processes (e.g. the effects of disturbance) or the geographical detail of the models represented in Figures 3 and 4. Furthermore, in the intercomparison the terrestrial components were calibrated to match the central estimate of the global carbon balance in the 1980s with an CO_2 emission from changing land use over the 1980s -- referred to as Dn80s in the IPCC SAR -- [*Schimel et al.*, 1996; *Wigley et al.*, 1997], of 16 GtC. This intercomparison yielded CO_2 concentration projections in 2100 ranging from 668 to 734 ppm, a range of width 66 ppm compared to a range of 164 ppm for the ISAM results presented here and in the IPCC TAR. Illustrated results in the IPCC SRRF were those of the Bern model [*Siegenthaler and Joos*, 1992] that gave 688 ppm in 2100.

The IPCC SAR [*Schimel et al.*, 1996] revised the projections given in the Special Report, in response to a revised 1980s carbon budget. The IPCC SAR 1980s budget had a CO_2 emission from changing land use over the 1980s of 11 GtC. When the strength of the CO_2 fertilization effect in the Bern model was weakened to match this 1980s budget, the CO_2 concentration projection in 2100 increased to 712 ppm. The sensitivity of IS92a results to the IPCC SAR calibration procedure was evaluated in an IPCC Technical Paper [*Wigley et al.*, 1997]. The parameterization of the ISAM model used for the IPCC SAR

(with climate effects on carbon cycle neglected) gave a similar CO_2 concentration projection in 2100 of 715 ppm (see Fig. 7b for SAR result). When the strength of the CO_2 fertilization effect was calibrated to match Dn80s = 18 to 4 GtC, CO_2 concentration projections in 2100 ranged from 667 to 766 ppm, a range of width 99 ppm -- still narrower than presented here. The range of projected temperature increase between 1990 and 2100 quoted from the IPCC SAR based on the range of IS92 scenarios is 1.0 to 3.5 ^{o}C, narrower than the range of temperatures presented here for only one (near the center) emission scenario, IS92a. Note that all reported temperature projections by the IPCC use modeled histories of past temperature; in this study we use observation-based temperatures for the past. While this difference in approach will have little effect on projections of temperature anomaly relative to preanthropogenic temperature, it will have an effect on the anomaly relative to 1990 since the IPCC's modeled histories do not match the observation-based temperatures for the range of parameters considered. Of course, climate models can and have been calibrated to match the observation based history [*Mitchell et al.*, 2001], however, this was not explicitly done in making the IPCC projections compared to here.

In the IPCC TAR, CO_2 concentration projection of both the ISAM model (with parameters described here and projections as included here) and the Joos et al. [2001] model were illustrated. As opposed to the meta-model approach adopted here, the

projections based on the Joos et al. [2001] model specified ranges of model input parameters that were thought to be the outer limits of possible parameter ranges. If indeed these are the outer limits, and if ranges of all relevant uncertain parameters are included, then that range would represent an upper bound on the range of projected CO_2 concentration (of course under the specifications of the scenario: emissions and certain radiative forcing from radiative forcing agents other than CO_2). Indeed, the IS92a CO_2 concentration projection of the Joos et al. [2001] model are wider, 703 (632 - 902) ppm by 2100, than the ISAM projections presented here and in the IPCC TAR.

Recent projections include varied results. In the DGVM intercomparison described in Section 2.2, nominally a simulation of the IS92a scenario based on results from the Hadley Centre, the specified CO_2 concentration in 2100 was 790 ppm [*Cramer et al.*, 2001], near the high end of the ISAM range. Furthermore, Cox et al. [2000] find that with a global carbon cycle model including a variant of the TRIFFID model when combined with another Hadley Centre climate model (HADCM-3) and climate drivers (no aerosols), but still nominally for the IS92a scenario (no land use change), led to considerably less accumulation of carbon in soils than would be represented by the range of ISAM meta-model results. Over the period from 2000 through 2099, Cox et al. [2000] reported plants and soils were a source of CO_2 rather than a sink as given in Table 2, and

led to a CO_2 concentration projections in 2100 of 980 ppm, above the range presented here and near the top of the range presented from the Joos et al. [2001] model.

Projections of CO_2 made with different parameterizations of the ISAM model in response to emission scenario IS92a are compared in Figure 7b and Table 2. This range of results corresponds to Dn80s of 0.9 (2.0 - 0.2) GtC/yr. The size of terrestrial uptake in the 1980s is not, however, highly coupled to the uptake over the next century -- due to decadal variability in terrestrial uptake as is evident in Fig. 3 -- and so the estimate of emissions from land use provide a weak constraint. These results include climate feedbacks on both the terrestrial and ocean (only the effect temperature on CO_2 solubility) responses resulting in a decrease in carbon uptake of both. Even so the reference ISAM CO_2 projection is still approximately identical that of the IPCC SAR, since CO_2 fertilization is that much stronger over the next century than in the IPCC SAR reference projection. If climate feedbacks are neglected in the ISAM model, then the reference result is even lower. Nevertheless, both the IPCC SAR and the no-climate-feedback reference projections are well within the range of projections representing the range of alternative model results.

Extending the initial time for projections from 1990, as used in the IPCC SAR and SRRF, to 1999 decreases the range of model projections in 2100. However, even

with this additional information and a further appreciation of terrestrial processes, we find the range of results to be wider than that in the IPCC SRRF [*Schimel et al.*, 1995].

The range of model results does provide information about uncertainty of future projections. While the set of ocean and terrestrial models used to calibrate the reduced form model still contain some representations of processes that are far from realistic (e.g. the incorporation of the effects of land use change and management, and nitrogen cycle), their results are, nevertheless, conceivable responses of CO_2 to emissions. If these model results are considered as a forecast of CO_2 concentration given a scenario of emissions, then the uncertainty range of that forecast must encompass the full range of model results, although the *true* response of the Earth system might lie outside of this range. Therefore, the range of these model results forms a lower bound on the range of uncertainty of the forecast. There are additional factors that could increase the range of conceivable projections and thus increase this lower bound on the uncertainty estimate. They include, for example, the effect of uncertain patterns of precipitation (not represented in the DGVM intercomparison in Figures 3 and 4), shifts in ocean circulation (not represented in ISAM results), and the effects of aerosols and other greenhouse gases (while the central estimate of radiative forcing virtually cancels globally for IS92a, this estimate is highly uncertain and can lead to patterns of climate change that will effect the terrestrial response).

4.2. SRES Scenarios

A set of 40 emission scenarios was reported in the IPCC Special Report on Emission Scenarios (SRES) [*Nakicenovic et al.*, 2000] and was intended to improve on the earlier set of 6 scenarios that include the IS92a benchmark considered in Section 4.1. These are scenarios intended not to include emission controls to limit climate change, sometimes referred to as *non-intervention* scenarios. Future emissions of greenhouse gases and aerosols are determined by driving forces such as population, socio-economic development and technological change, and hence are highly uncertain. The 40 SRES scenarios consist of six scenario groups, based on narrative storylines, which span a wide range of these driving forces. They encompass four combinations of demographic change, and social and economic development (scenario groups labeled A1, A2, B1, B2). Scenario group A1 is further split into three scenario groups, A1B, A1FI and A1T, that explicitly explore alternative directions for energy technology in the energy system. In this study we consider only the 6 scenarios -- labeled marker or illustrative scenarios in the IPCC SRES [*Nakicenovic et al.*, 2000] -- that are illustrative of the 6 groups.

Fossil carbon dioxide emissions for these 6 SRES scenarios are summarized in Table 2 and Fig. 8a. The B1 and A1 scenarios are based on a low projection of future global population with 7 billion people in 2100 after having reached a maximum of 9 billion earlier during the century, whereas the B2 and A2 scenarios follow medium and high projections, respectively. The two scenarios with the lowest CO_2 emissions are the

B1 scenario characterized by a storyline emphasising environmental and societal sustainability, and the A1T scenario characterized by a storyline emphasising rapid economic growth along with rapid development and implimentation of non-fossil energy sources. The scenario with most rapidly increasing emissions, A1FI, on the other hand, is characterised by a storyline emphasising rapid economic growth and carbon-intensive energy supply systems, whereas the A1B storyline has a *balance* between non-fossil and fossil energy systems. The A2 storyline is on of a world with economic development regionally oriented with slow economic growth. The B2 storyline has intermediate levels of economic growth with less rapid technological development than A1 or B1.

The SRES scenarios also include emissions of greenhouse gases in addition to CO_2 as well as the aerosol precursor SO_2. To model the effect on the climate/carbon cycle system, we adopt the contributions of non-CO_2 greenhouse gases and aerosols to the total radiative forcing of climate listed in the IPCC TAR [*Ramaswamy et al.*, 2001]. It is important to note these contributions do not include an appreciable net contribution from non-sulfate aerosols, do not include any radiative forcing from land cover change, and do not account for any natural variations in radiative frocing (e.g. future volcanoes and solar variations could contribute to future radiative forcing and, if not predictable, further contribute the range of uncertain in forecasts of future climate). Furthermore, the uncertainty in the radiative forcing effect of aerosols, which is not well characterized [*Ramaswamy et al.*, 2001], in particular is a primary contributor to the uncertainty in radiative forcing [*Schwartz and Andreae*, 1996] and has been explained to be a barrier in both the detection of an enhanced greenhouse gas effect in climate records and

quantitative forecasts of future climate. Neglecting these uncertainties, as is done here and in the climate change projections of the IPCC Third Assessment Report [*Cubasch et al.*, 2001] misses an important contributor to the uncertainty in climate projections to be considered when drawing implications of these climate change projections.

A heavily communicated feature of the IPCC TAR [2001b] was the higher range (1.4 to 5.8 ^{o}C) of projected global temperature increase from 1990 to 2100 than had been reported (1.0 to 3.5 ^{o}C) in the IPCC SAR [*Kattenburg et al.*, 1996]. The cause of the higher projections was the lower emission rates of SO_2, a precursor to sulfate aerosols modeled to be a global cooling agent, specified in the SRES scenarios compared to the scenarios [*Leggett et al.*, 1992] used to make the IPCC SAR projections. The reason for reducing the SO_2 emission rate in the SRES scenarios was the expectation that SO_2 emission controls would be stronger than assumed in the previous set of scenarios [*Nakicenovic et al.*, 2000]. While the SRES scenarios were not intended to include emission reductions for the purpose of climate change mitigation, they were intended to include reductions to control pollutants. But, while SO_2 emissions were lowered in SRES, tropospheric ozone precursor emissions were not; since tropospheric ozone is a gobal warming agent, the seemingly inconsistent reduction of the cooling agent SO_2 without the control of tropospheric ozone results in a higher range of temperature projections than if tropospheric ozone were also controlled [*Wigley and Raper*, 2001]. This led the IPCC [2001a] to conclude that a key uncertainty in future projections is "Inadequate emission

scenarios for ozone and aerosol precursors". In addition the IPCC [2001a] concluded another key uncertainty in future projections are "Factors in modeling of carbon cycle including the effects of climate feedbacks"; we begin to address this factor next.

The projected range of CO_2 response to the 6 SRES scenarios is made using the alternative -- reference (low and high CO_2) -- parameterizations of the ISAM model in the same way as with the IS92a scenario (Section 4.1). The CO_2 response is calculated starting from the initial condition in 1999. Observation-based estimates of fossil emissions through 1999 are used to calculate the initial condition, and beginning in 2000 SRES emissions are specified.

Projected CO_2 concentrations are presented in Figure 8b and carbon budgets in Table 2. The alternative CO_2 concentration projections for the different model parameterizations of all 6 scenarios overlap to some extent up until 2050. Scenario A1FI results in the highest projected CO_2 concentration in 2100 of 970 (851 - 1,062) ppm, followed by A2, A1, B2, A1T and B1. The lowest, scenario B1, results in a projected CO_2 concentration of 549 (490 - 603) ppm in 2100. The range of projections in 2100 for any one scenario is, therefore, 27 to 50% as wide as the range of reference projections for the 6 different scenarios. If these ranges are representative of the magnitude of uncertainty in *1)* future emissions and *2)* our ability to predict the response of CO_2 to emissions, then both of these contributors to uncertainty would be significant if the

ultimate goal were to manage emissions to reach a CO_2 concentration targets over the next century. These results in no way indicate, however, that higher emissions might lead to lower concentrations; higher emissions lead to higher projected concentrations for projections of every model considered over this time scale. The range of projected CO_2 concentrations for the different ISAM parameterizations is primarily due to the modeled range of the change in carbon stocks in plants and soils: see Table 2. This range of reference projections, 549 to 970 ppm in 2100, is slightly higher than the range of reference projections (made with the Bern model) of the IS92 scenarios given in the SAR of 488 to 944 ppm [c.f. *Wigley*, 1999]. Tabulated values of projected CO_2 concentrations and the related radiative forcing estimates are listed in Appendix II of the IPCC TAR [*IPCC*, 2001b].

Projected global mean temperature anomalies are presented in Figure 8c. Scenario A1FI results in the highest projected global mean temperature anomaly in 2100 of 4.7 (2.8 - 7.5) ^{o}C, followed by A2, A1, B2, A1T and B1. The lowest, scenario B1, results in a temperature anomaly of 2.4 (1.3 - 4.1) ^{o}C. The difference between the projected global temperature anomaly in 2100 and the observation-based anomaly in 1990 (0.68 ^{o}C) is, therefore, 4.0 (2.1 - 6.8) ^{o}C for A1FI and 1.7 (0.6 - 3.4) ^{o}C for B1 -- an overall range for the 6 SRES scenarios of 0.6 to 6.8 ^{o}C.

The range of projected temperature increase from 1990 to 2100 in this analysis (0.6 to 6.8 ^{o}C) is wider than the range (1.4 to 5.8 ^{o}C) highlighted in the IPCC TAR

[*Cubasch et al.*, 2001]. Furthermore, the IPCC TAR based its range on the full set of 40 SRES scenarios (5 of the 40 were not analyzed because they did not include as many greenhouse gases than the others, although their cumulative CO_2 emissions were within the range of the remaining 35 and would not expand the range of projected CO_2 concentration or temperature) and the 40 SRES scenarios had a somewhat wider range of cumulative CO_2 emissions than the 6 marker/illustrative scenarios considered in this analysis. There are several reasons for the wider range of temperature projections in this study:

1. A wider range of CO_2 concentration projections is found in this study for the 6 SRES scenarios than was used in the IPCC TAR for the 35 SRES scenarios analyzed [*Wigley and Raper*, 2001]. The wider CO_2 projection range in this study is due to the range of modeled carbon cycle response to a given emission scenario, a contributor to uncertainty not included in the IPCC TAR temperature projections [*Cubasch et al.*, 2001].

2. A wider range of climate sensitivity, $\Delta T_{2x} = 1.5^{o}C$ to $4.5^{o}C$, is assumed in this study than in the IPCC TAR where $\Delta T_{2x} = 1.7^{o}C$ to $4.2^{o}C$ [*Cubasch et al.*, 2001].

3. Finally, in this study temperature change is measured relative to the observation-based estimate of global temperature in 1990, instead of the modeled estimate of 1990 temperature. In this study, the energy balance

model is forced to match the observation-based estimate of global temperature through 1999, whereas the IPCC TAR analysis gives past global temperatures based on an energy balance model with a scenario of past radiative forcing (since past radiative forcing from, e.g., aerosols is highly uncertain). This difference in methodology adds to a wider range of temperature change in this study than in the IPCC TAR.

The range of temperature projections depends on the method for producing that range, which has differed between previous assessments, which also differ from this analysis. Inferring shifts in the risk assessment of climate change from such shifts in projected temperature range should take into account shifts in the methodology used to make projections.

4.3. Analysis of Stabilization of CO_2 Concentration

In this section, emission rates of CO_2 that arrive at various stable CO_2 concentration levels are estimated using a similar methodology as is used in analyses of emission scenarios. The set of five different CO_2 trajectories, defined by Wigley et al. [1996] shown in Figure 9a is analyzed. These trajectories were designed to follow CO_2 concentration consistent with the IS92a emission scenario beginning in 1990, and

branching off to reach constant CO_2 concentrations of 450, 550, 650, 750, or 1000 ppm over the following centuries [*Wigley et al.*, 1996]. Justification for various alternative time trajectories, stabilization levels, and related emissions, have been considered in detail in the IPCC TAR [*Morita et al.*, 2001] requiring assessment of a range of socio-economic factors corresponding to future emission scenarios. This section is concerned with the estimation of *anthropogenic* (i.e. the sum of CO_2 emissions resulting from fossil carbon and land use) emissions given specific CO_2 concentration trajectories, which is fundamentally a natural science question.

The three alternative parameterizations (reference, low CO_2, and high CO_2) of the ISAM model are used to calculate the ocean and terrestrial CO_2 uptake resulting from the prescribed change in CO_2 concentration. Since CO_2 is prescribed , the change in climate can be calculated uncoupled from either the ocean or terrestrial carbon cycle models. As in the emission scenario analyses in Section 4.1-2, observation-based global temperature and CO_2 are specified through 1999. From 2000 onward, global temperature is calculated from CO_2 radiative forcing only. The effects of aerosols and other greenhouse gases are neglected in these calculations since these roughly cancel each other (on a global scale) in the IS92a scenario up to 2100, and scenarios have not been associated with these CO_2 trajectories after 2100. The alternative parameterizations yield a range of climate projections. With CO_2 and global temperature defined in this way the ocean and

terrestrial carbon cycle model components are also uncoupled from each other and can be calculated independently for the three alternative parameterizations. Note that in these cases, land use emissions are specified to follow the IS92a scenario until 2100, and are assumed to be zero thereafter. From the carbon budget, fossil emissions are equated to the calculated accumulation rate of carbon in the atmosphere, oceans, plus the terrestrial biosphere (including land use emissions).

The results of these calculations are given in Table 3 and Figure 9. As with results for the emission scenarios in Sections 4.1 and 4.2, results for the reference parameterization are not substantially different than those reported in the IPCC SAR [*Schimel et al.*, 1996], which were calculated with the Bern model [*Siegenthaler and Joos*, 1992]. Again the range of ISAM results -- in this case *anthropogenic* CO_2 emissions -- for the alternative parameterizations is wider than the range presented in the IPCC SRRF [*Schimel et al.*, 1995] but narrower than the results presented in the IPCC TAR using the Joos et al. [2001] model. For example, the ranges of *anthropogenic* emissions for the CO_2 trajectories leading to 450 ppm and 1,000 ppm overlap until 2040.

Table 3 shows the modeled carbon budgets based on the different ISAM parameterizations applied to the stablization CO_2 trajectories. Changes in carbon stocks of plants and soils, the oceans, the atmosphere, and fossil carbon are aggregated over each of the next three centuries. Since the change in atmospheric CO_2 is specified, the

change in atmospheric carbon content is independent of the model parameterization. Once a constant CO_2 concentration is reached (see Figure 9a), the change in atmospheric carbon stock becomes zero. Note that the low CO_2 ISAM parameterization corresponds to the high extreme of the increase in plant and soil, and ocean carbon stocks along with the greatest decrease in fossil carbon stocks; the converse is the case for the high CO_2 ISAM parameterization while the reference case lies in between. Over the period from 2000 to 2099, increase in carbon stocks by the oceans is larger than -- but of comparable magnitude to -- that of plants and soils. The range of carbon accumulation in plants and soils is, however, somewhat wider than that of the oceans accounting for the majority of the range of deduced fossil fuel emissions. Over the next two centuries, this pattern changes. Over the period from 2200 to 2299, increase in carbon stocks by the oceans is far larger than that of plants and soils, which in some cases is negative (a net source of CO_2). Furthermore, the range of carbon accumulation (caused by different model parameterizations) in plants and soils decreases in relation to that of the oceans.

One artifact of these cases is that the range of land use emission prior to year 2000 does not match that specified exactly in scenario IS92a, and the CO_2 concentration trajectories (Fig. 9a) were constructed with a different carbon cycle model. Consequently, the estimated fossil emissions following 1999 are discontinuous with the observation-based estimate of fossil emissions in 1999. In Figure 9b and in the IPCC TAR [*Prentice et al.*, 2001] *anthropogenic* CO_2 emissions are presented obscuring this artifact. Further consideration of appropriate ways of including uncertain land use emissions in CO_2 stabilization studies is needed to address this artifact [c.f. *Bolin and Kheshgi*, 2001].

Temperature anomaly is calculated from the prescribed CO_2 stablization trajectories: see Figure 9c. In these calculations radiative forcing from only CO_2 is included. Since CO_2 concentrations are specified, the temperature results are uncoupled from carbon cycle and do not depend on carbon cycle behavior, although carbon cycle remains couple to climate. The range in temperature projections for a given CO_2 stablization trajectory in this analysis depends primarily on the climate sensitivity ΔT_{2x}. The temperature range for a CO_2 stablization trajectory -- e.g. stabilizing at 550 ppm as shown in Figure 9c -- is comparable in width to the range of reference temperature projections over the span of stabilization levels -- 450 to 1,000 ppm.

We note that the calibration of ISAM for use as a meta-model was carried out in Section 3 only for a scenario lasting one century, not the longer period considered for the stabilization of CO_2 concentration. Furthermore, interactions between ocean circulation/mixing and climate were not included, and these do become an important factor in slowing the ocean uptake of CO_2 after about 2050 in model studies [*Sarmiento et al.*, 1998; *Joos et al.*, 1999; *Prentice et al.*, 2001], although they have yet to be included in scenario analyses and the integrated assessment of climate change. Therefore, the information contained in the model intercomparisons that are the basis for the use of ISAM as a meta-model may well be insufficient for the analysis of stabilization of CO_2, which spans several centuries.

To maintain a constant future CO_2 concentration, net anthropogenic CO_2 emissions would ultimately need to be reduced to the size of persistent natural sinks enhanced due to, for example, the enhanced CO_2 concentration. Modeled sinks caused by enhanced growth of plants, and carbon accumulation in soils due to increased CO_2 is

important over a century time-scale as seen in the DGVM intercomparison in Section 3 [*Cramer et al.*, 1999]. Beyond a century, terrestrial sinks are not well understood. Mixing of ocean disolved inorganic carbon between surface and deep waters is modeled to continue to lead to ocean uptake with an exponential decay time-scale of several centuries following a change in atmospheric CO_2 [*Maier-Reimer and Hasselmann*, 1987; *Sarmiento et al.*, 1992]. This mixing is the primary factor responsible for the continued ocean uptake, and calculated *anthropogenic* CO_2 emissions following CO_2 stabilization in the cases analyzed here as show in the carbon budget in Table 3 and in Fig. 9b. The primary known enhanced natural sink expected to persist beyond the mixing time of the oceans is that due to dissolution of $CaCO_3$ in ocean sediments, which increases ocean alkalinity thereby allowing additional CO_2 to dissolve in the oceans. For CO_2 concentration levels up to 1,000 ppm, this sink is estimated to be on the order of 0.1 GtC/yr [*Archer et al.*, 1998]. For the range of stabilization cases analyzed in this section, the net *anthropogenic* CO_2 emissions would ultimately decrease to the order of 0.1 GtC/yr unless currently unknown sinks are discovered. This does not, however, preclude the possibility of the engineering of long-term anthropogenic sinks of carbon.

5. Concluding Discussion

5.1. Methodology

The accuracy and uncertainty of projections of future climate change is the central question for the science of climate change. Assessments of climate change carried out by the IPCC have primarily used ranges of model results as a measure of the uncertainty of projections, given scenarios for human activities. This approach has characteristics that we consider below in relation to the results presented in this paper.

Including ranges of behavior of additional components of the climate system increases the range of results for the integrated system: In this study, we used a simple Earth system model to combine ranges of behavior of the ocean, terrestrial biosphere, and climate systems to compute ranges of behavior of the integrated system. Including ranges of model results for each component increases the range of integrated system. For example, in the IPCC SRRF [*Schimel et al.*, 1995] and SAR [*Schimel et al.*, 1996] CO_2 projections, effects of changing climate on carbon cycle were not included, which is a partial cause for the narrower ranges of CO_2 projections seen in those assessments compared to the IPCC TAR [*Prentice et al.*, 2001]. Including the range of the modeled carbon cycle system increases the range of projected global temperature to be even wider than that communicated by the Third Assessment Report of the IPCC. Furthermore,

there are further contributors to uncertainty that were not included in this study. These included, e.g. ranges of aerosol and non-CO_2 radiative climate forcing, natural climate forcing factors, change in ocean transport, effects of nitrogen fertilization of plants and soils, and scientific uncertainty in relating land use effects on carbon cycle and climate. Including these factors would further increase the range of integrated system results.

Including outlying models in the set of models that define a range of projections increases the range: The envelope of alternative model simulations, if plausible responses, must be contained within the uncertainty range. Therefore, including additional model results can only increase an uncertainty range estimated only by considering the range. Beyond the range of carbon cycle and climate model results represented by the ISAM meta-model in this study, additional results have appeared. For example, Cox et al. [2000] find that a variant of the TRIFFID model, when combined with a different climate model and climate drivers (no aerosols) than was considered TRIFFID's use in Cramer et al. [2001] led to considerably less accumulation of carbon in soils than would be represented by the range of ISAM meta-model results. This might be an artifact of the way the meta-model was parameterized to match the range of DGVMs given the limited information on modeled mechanisms for the behavior of the simulations. Nevertheless, if the Cox et al. [2000] simulation were spanned by the range of the meta-model, the range of projections would extend to even higher temperatures

and CO_2 concentrations. In addition, for example, if the alternative mechanism for interactions between cirrus clouds and climate as proposed by Lindzen et al. [2001] were included, then the range of climate sensitivity would be extended to lower values and the range of projections would extend to even lower temperatures and CO_2 concentrations. Since model intercomparisons will not include all plausible responses of the system, their range may underestimate uncertainty.

Tests for plausibility of component models in intercomparisons: If model results are found to be implausible, then they would not be considered in the range for modeling the intergrated system. However, the grounds for inclusion of model results in model intercomparisons, and their use in defining assessed ranges of behavior, is often not transparent, and may be restrictive in terms of their model structure (e.g. using only DGVM results in this study). Transparent grounds for model consideration and rejection are needed.

Observational constraints on integrated system results: Past behavior of the Earth system does provide constraints on the range of the integrated system response. For example, in an earlier study using ISAM [*Kheshgi et al.*, 1999; *Kheshgi and Jain*, 2000], observational constraints were used to estimate a range of Earth system model parameters. Ranges of model parameters generated from model intercomparisons could,

in principle, be used to define prior ranges of model parameters. Bayesian statistical estimation could then be used to apply observational constraints. There are many aspects of this kind of analysis that would need to be addressed: e.g., characterization and inclusion of variability in both climate and carbon cycle, observational uncertainties, all relevant factors in past climate change, and model structure effects on the relationship between past and future model behavior. Clearly, further work is needed to apply observational constraints on the integrated system in an appropriate manner. Nevertheless, observational constraints do hold some potential for limiting uncertainty in projections.

Assignment of probability to ranges of projections: Many of the issues in the use of model intercomparisons for the estimation of uncertainty in projections could be avoided if it were possible to assign probabilities to each of the alternative model responses, that is the probability that an alternative is the *true* outcome. The high profile result of the IPCC TAR [*IPCC*, 2001b] was a higher range of projected global temperature increase over the next century -- 1.4 to 5.8 °C -- than was assessed in the IPCC SAR [*IPCC*, 1996] -- 1.0 to 3.5 °C (c.f. projections in Section 4.2). However, no probability was assigned in the IPCC TAR to this range, bringing into question the usefulness of this range in characterizing the risk of global climate change [*Reilly et al.*, 2001; *Schneider*, 2001; *Wigley and Raper*, 2001] and our ability to assign probabilities [*Allen et al.*, 2001;

Grubler and Nakicenovic, 2001]. Doing so remains a highly subjective exercise [*Morgan and Keith*, 1995]. In studies [*Schneider*, 2001; *Wigley and Raper*, 2001] where probabilities were assigned to alternative emission scenarios and models, a narrow probability distribution was found partially due to the specification that these factors are statistically independent. Furthermore, Wigley and Raper [2001] found that the contribution to the probability distribution of uncertainty in carbon cycle was negligible due to its effects being weakly correlated to climate in their model of the Earth system, and the fact that in combinations of uncorrelated uncertain factors the contribution of the largest contributors dominates (e.g. as seen in taking the root mean square). This is in contrast to the wider range of temperature projections given in Section 4.2 due largely to the larger range in CO_2 concentration from the range of carbon cycle response. While this range might be muted if probabilities are assigned, the stronger correlation between temperature and carbon cycle exhibited in this model than in that used by Wigley and Raper [described in *Cubasch et al.*, 2001] may leave carbon cycle uncertainty as a significant contributor based on ISAM. The strength of the climate feedback on carbon cycle, and the corresponding correlation between climate and CO_2, continues to differ considerably in alternative studies [e.g. *Cox et al.*, 2000; *Friedlingstein et al.*, 2001].

5.2. Key Results

1. DGVMs exhibit a stronger increase in CO_2 uptake in response to enhanced CO_2 levels than assessed in the IPCC SAR [*Schimel et al.*, 1996]. DGVMs exhibit a decrease in CO_2 uptake in response to a warming climate scenario. Trends in DGVM CO_2 uptake, and their dependence on CO_2 and temperature, are simulated by ISAM (see Section 2.1).
2. Detailed ocean models continue to exhibit a CO_2 uptake response to enhanced CO_2 levels comparable to the IPCC SAR [*Schimel et al.*, 1996] with little climate effect via circulation change over the next 50 years. In this study the range of ocean model behavior is simulated by ISAM and the effect of temperature on CO_2 solubility is included (see Section 2.2).
3. Model reconstruction of CO_2 ocean uptake over the 1980s and 1990s (see Section 3), when forced by the observed warming which is strong over these decades, gives an ocean uptake that is about 0.3 GtC/yr lower than when the temperature effect on CO_2 solubility is neglected, as was done in the IPCC SAR [*Schimel et al.*, 1996] and the IPCC Special Report on Land Use, Land Use Change and Forestry [*Bolin et al.*, 2000].
4. Observed terrestrial carbon uptake over a single decade is found to be of limited use to calibrate terrestrial carbon cycle models until the potentially strong decadal variability in terrestrial CO_2 uptake is understood (see Section 2.2).

5. Model-based carbon budgets over the past century match observation-based budgets of ocean CO_2 uptake and land use emissions (see Section 3).
6. In the benchmark future emission scenario IS92a (see Section 4.1), modeled climate feedback compensates for a stronger CO_2 fertilization effect resulting in nearly identical projections, in the reference case, as in the IPCC SAR [*Schimel et al.*, 1996]. The range width of model results, however, is 164 ppm in 2100 -- wider than considered in past assessments [*Schimel et al.*, 1995].
7. A similar range of CO_2 projections (see Section 4.2) is found for the IPCC SRES emission scenarios as is found for the IS92a emission scenario; the consequent range of global temperature projections is wider than that highlighted by the IPCC [2001b], although probabilities are not assigned to this range [c.f. *Wigley and Raper*, 2001].
8. Model projections of CO_2 emissions leading to stable CO_2 concentrations (see Section 4.3) show a range of anthropogenic CO_2 emissions wide enough to obscure the emission pathways leading to different CO_2 concentration levels (see Fig. 9b), although to a lesser extent than projections of global temperature (see Fig. 9c).

6. Acknowledgements

We wish to acknowledge Martin Heimann, Colin Prentice and Corine Lequere for suggestions and facilitation of the aquisition of model intercomparison results. We

acknowledge Wolfgang Cramer, Jim Orr and the many contributors of results to the model intercomparison projects. And we acknowledge Fortunat Joos for providing radiative forcing contributions from non-CO_2 greenhouse gases and aerosols as used in this IPCC TAR.

References

Allen, M., S.C.B. Raper and J. Mitchell, Uncertainty in the IPCC's Third Assessment Report, *Science*, *293*, 430-433, 2001.

Archer, D., H. Kheshgi and E. Maier-Reimer, The dynamics of fossil fuel CO_2 neutralization by marine $CaCO_3$, *Global Biogeochemical Cycles*, *12*, 259-276, 1998.

Archer, D.E., T. Takahashi, S. Sutherland, J. Goddard, D. Chipman, K. Rodgers and H. Ogura, Daily, seasonal and interannual variability of sea-surface carbon and nutrient concentration in the equatorial Pacific Ocean, *Deep-Sea Research Part II-Topical Studies in Oceanography*, *43*, 779-808, 1996.

Bolin, B. and H.S. Kheshgi, On strategies for reducing greenhouse gas emissions, *Proceedings of the National Academy of Sciences of the United States of America, 98,* 4850-4854, 2001.

Bolin, B., R. Sukumar, P. Ciais, W. Cramer, P. Jarvis, H. Kheshgi, C. Nobre, S. Semenov and W. Steffen, Global Perspective, in *Land Use, Land-Use Change, and Forestry: A Special Report of the Intergovernmental Panel on Climate Change*, edited by R.T. Watson et al., pp. 23-51, Cambridge University Press, New York, 2000.

British Petroleum Company, *BP Statistical Review of World Energy 1999*, British Petroleum Company, London, 2000.

Brovkin, V., A. Ganopolski and Y. Svirezhev, A continuous climate-vegetation classification for use in climate-biosphere studies, *Ecological Modelling*, *101*, 251-261, 1997.

Cox, P.M., R.A. Betts, C.D. Jones, S.A. Spall and I.A. Toterdell, Acceleration of global warming due to carbon-cycle feedbacks in a coupled climate model, *Nature*, *408*, 184-187, 2000.

Cramer, W., A. Bondeau, F.I. Woodward, I.C. Prentice, R.A. Betts, V. Brovkin, P.M. Cox, V. Fisher, J.A. Foley, A.D. Friend, C. Kucharik, M.R. Lomas, N. Ramankutty, S. Sitch, B. Smith, A. White and C. Young-Molling, Global response of terrestrial ecosystem structure and function to CO2 and climate change: results from six dynamic global vegetation models, *Global Change Biology*, *7*, 357-374, 2001.

Cramer, W., D.W. Kicklighter, A. Bondeau, B. Moore˙III, G. Churkina, B. Nemry, A. Ruimy and A.L. Schloss, Comparing global models of terrestrial net primary

productivity (NPP): Overview and key results, *Global Change Biology, 5 (Suppl. 1)*, 1-15, 1999.

Cubasch, U., G.A. Meehl, G.J. Boer, R.J. Stouffer, M. Dix, A. Noda, C.A. Senior, S. Raper and K.S. Yap, Projections of future climate change, in *Climate Change 2001: The Scientific Basis: Contribution of WGI to the Third Assessment Report of the IPCC*, edited by J.T. Houghton et al., pp. 525-582, Cambridge University Press, New York, 2001.

DeFries, R.S., C.B. Field, I. Fung, G.J. Collatz and L. Bounoua, Combining satellite data and biogeochemical models to estimate global effects of human-induced land cover change on carbon emissions and primary productivity, *Global Biogeochemical Cycles, 13*, 803-815, 1999.

Enting, I.G., T.M.L. Wigley and M. Heimann, Eds., Future emissions and concentrations of carbon dioxide: Key ocean/atmosphere/land analyses, CSIRO Division of Atmospheric Research Technical Paper No. 31, Australia, CSIRO, 1994.

Feely, R.A., R. Wanninkhof, T. Takahashi and P. Tans, Influence of El Niño on the equatorial Pacific contribution to atmospheric CO_2 accumulation, *Nature, 398*, 597-601, 1999.

Foley, J.A., I.C. Prentice, N. Ramankutty, S. Levis, D. Pollard, S. Sitch and A. Haxeltine, An integrated biosphere model of land surface processes, terrestrial carbon balance, and vegetation dynamics, *Global Biogeochemical Cycles*, *10*, 603-628, 1996.

Friedlingstein, P., L. Bopp, P. Ciais, J.-L. Dufresne, L. Fairhead and H. LeTreut, Positive feedback between future climate change and the carbon cycle, *Geophysical Research Letters*, *28*, 1543-1546, 2001.

Friend, A.D., A.K. Stevens, R.G. Knox and M.G.R. Cannell, A process-based, terrestrial biosphere model of ecosystem dynamics (Hybrid v3.0), *Ecological Modelling*, *95*, 249-287, 1997.

Gruber, N., J.L. Sarmiento and T.F. Stocker, An improved method for detecting anthropogenic CO_2 in the Oceans, *Global Biogeochemical Cycles*, *10*, 809-837, 1996.

Grubler, A. and N. Nakicenovic, Identifying dangers in an uncertain climate, *Nature*, *412*, 15, 2001.

Harvey, L.D.D., Effect of model structure on the response of terrestrial biosphere models to CO_2 and temperature increases, *Global Biogeochemical Cycles*, *3*, 137-153, 1989a.

Harvey, L.D.D., Managing atmospheric CO_2, *Climatic Change*, *15*, 343-381, 1989b.

Harvey, L.D.D., J. Gregory, M. Hoffert, A. Jain, M. Lal, R. Leemans, S.C.B. Raper, T.M.L. Wigley and J.R. de Wolde, *An introduction to simple climate models used in*

the IPCC Second Assessment Report. IPCC Technical Paper II, Intergovernmental Panel on Climate Change, Bracknell, UK, 1997.

Heimann, M., G. Esser, A. Haxeltine, J. Kaduk, D.W. Kicklighter, W. Knorr, G.H. Kohlmaier, A.D. McGuire, J. Melillo, B. Moore, R.D. Otto, I.C. Prentice, W. Sauf, A. Schloss, S. Sitch, U. Wittenberg and G. Wurth, Evaluation of terrestrial carbon cycle models through simulations of the seasonal cycle of atmospheric CO2 - first results of a model intercomparison study, *Global Biogeochemical Cycles, 12*, 1-24, 1998.

Houghton, R.A., The annual net flux of carbon to the atmosphere from changes in land use 1850-1990, *Tellus, 50B,* 298-313, 1999.

Houghton, R.A., A new estimate of global sources and sinks of carbon from land-use change, *EOS, 81*, S281, 2000.

Huntingford, C., P.M. Cox and T.M. Lenton, Contrasting responses of a simple terrestrial ecosystem model to global change, *Ecological Modelling, in press*, 2000.

IPCC, *Climate Change 1995: the Science of Climate Change, Contribution of WGI to the Second Assessment Report of the Intergovernmental Panel on Climate Change,* Cambridge University Press, Cambridge, 1996.

IPCC, *Revised 1996 IPCC Guidelines for National Greenhouse Gas Inventories. Reference Manual,* Intergovernmental Panel on Climate Change, Geneva, 1997.

IPCC, *Climate Change 2001: Synthesis Report of the IPCC Third Assessment Report*, Cambridge University Press, New York, 2001a.

IPCC, *Climate Change 2001: The Scientific Basis: Contribution of WGI to the Third Assessment Report of the IPCC*, Cambridge University Press, New York, 2001b.

Jain, A. and K. Hayhoe, Global air pollution problems, in *Handbook of Atmospheric Sciences*, edited by C.N. Hewitt and A.V. Jackson, pp. in press, Blackwell Science Ltd., Oxford, UK, 2001.

Jain, A.K., H.S. Kheshgi, M.I. Hoffert and D.J. Wuebbles, Distribution of radiocarbon as a test of global carbon cycle models, *Global Biogeochemical Cycles*, *9*, 153-166, 1995.

Jain, A.K., H.S. Kheshgi and D.J. Wuebbles, *Integrated Science Model for Assessment of Climate Change*, Air & Waste Management Association, 94-TP59.08, 1994.

Jain, A.K., H.S. Kheshgi and D.J. Wuebbles, A globally aggregated reconstruction of cycles of carbon and its isotopes, *Tellus*, *48B*, 583-600, 1996.

Jones, P.D., D.E. Parker, T.J. Osborn and K.R. Briffa, Global and hemispheric temperature anomalies--land and marine instrumental records, in *Trends: A Compendium of Data on Global Change*, Oak Ridge National Laboratory, Oak Ridge, Tenn., U.S.A., 2000.

Joos, F., M. Bruno, R. Fink, U. Siegenthaler, T. Stocker, C. Le Quéré and J.L. Sarmiento, An efficient and accurate representation of complex oceanic and biospheric models of anthropogenic carbon uptake, *Tellus, 48B,* 397-417, 1996.

Joos, F., G.-K. Plattner, T. Stocker, O. Marchal and A. Schmittner, Global warming and marine carbon cycle feedbacks on future atmospheric CO2, *Science, 284,* 464-467, 1999.

Joos, F., I.C. Prentice, S. Sitch, R. Meyer, G. Hooss, G.-K. Plattner, S. Gerber and K. Hasselmann, Global warming feedbacks on terrestrial carbon uptake under the IPCC emission scenarios, *Global Biogeochemical Cycles, in press,* 2001.

Kattenburg, A., F. Giorgi, H. Grassl, G.A. Meehl, J.F.B. Mitchell, R.J. Stouffer, T. Tokioka, A.J. Weaver and T.M.L. Wigley, Climate models – projections for future climate, in *Climate Change 1995: The Science of Climate Change: Contribution of WGI to the Second Assessment Report of the IPCC,* edited by J.T. Houghton et al., pp. 285-357, Cambridge University Press, New York, 1996.

Keeling, C.D., The carbon dioxide cycle: Reservoir models to depict the exchange of atmospheric carbon dioxide with the oceans and land plants, in *Chemistry of the Lower Atmosphere,* edited by S.I. Rasool, pp. 251-329, Plenum, NY, 1973.

Keeling, C.D. and T.P. Whorf, Atmospheric CO_2 records from sites in the SIO air sampling network, in *Trends: A Compendium of Data on Global Change,* Carbon

Dioxide Information Analysis Center, Oak Ridge National Laboratory, Oak Ridge, Tenn., U.S.A., 2000.

Kheshgi, H.S. and A.K. Jain, Uncertainty in projected CO2 responses to future emission scenarios (abstract), *Eos Trans. AGU, 81*, S17, 2000.

Kheshgi, H.S., A.K. Jain and D.J. Wuebbles, Accounting for the missing carbon sink with the CO_2 fertilization effect, *Climatic Change, 33*, 31-62, 1996.

Kheshgi, H.S., A.K. Jain and D.J. Wuebbles, Model-based estimation of the global carbon budget and its uncertainty from carbon dioxide and carbon isotope records, *J. Geophys. Res., 104*, 31,127-31,144, 1999.

Kheshgi, H.S. and B.S. White, Modelling ocean carbon cycle with a nonlinear convolution model, *Tellus, 48B*, 3-12, 1996.

Le Quéré, C., O. Aumont, L. Bopp, P. Bousquet, P. Ciais, R. Francey, M. Heimann, R. Keeling, H. Kheshgi, P. Peylin, S. Piper, I.C. Prentice and P. Rayner, *Two decades of ocean CO2 sink and variability* 6th International CO2 Conference, October 1-5, Sendai, Japan, 2001.

Le Quéré, C., J.C. Orr, P. Monfray and O. Aumont, Interannual variability of the oceanic sink of CO2 from 1979 through 1997, *Global Biogeochemical Cycles, 14*, 1247-1265, 2000.

Leggett, J., W.J. Pepper and R.J. Swart, Emission scenarios for the IPCC: an update, in *Climate Change 1992: The Supplementary Report to the IPCC Scientific Assessment*, edited by J.T. Houghton, B.A. Callander and S.K. Varney, pp. 69-96, Cambridge University Press, New York, 1992.

Levitus, S., J. Antonov, T.P. Boyer and C. Stephens, Warming of the world ocean, *Science, 287*, 2225-2229, 2000.

Lindzen, R.S., M.-D. Chou and A.Y. Hou, Does the Earth have an infrared iris?, *Bull. Amer. Meteor. Soc., 82*, 417-432, 2001.

Maier-Reimer, E. and K. Hasselmann, Transport and storage of CO_2 in the ocean—An inorganic ocean-circulation carbon cycle model, *Clim. Dyn., 2*, 63-90, 1987.

Marland, G., T.A. Boden and R.J. Andres, Global, regional, and national CO_2 emissions, in *Trends: A Compendium of Data on Global Change*, Carbon Dioxide Information Analysis Center, Oak Ridge National Laboratory, U. S. Department of Energy, Oak Ridge, Tenn., U.S.A., 2000.

Mitchell, J.F.B., T.C. Johns, J.M. Gregory and S.F.B. Tett, Climate response to increasing levels of greenhouse gases and sulphate aerosols, *Nature, 376*, 501-504, 1995.

Mitchell, J.F.B., D.J. Karoly, G.C. Hegerl, F.W. Zwiers, M.R. Allen and J. Marengo, Detection of climate change and attribution of causes, in *Climate Change 2001: The Scientific Basis: Contribution of WGI to the Third Assessment Report of the IPCC,* edited by J.T. Houghton et al., pp. 695-738, Cambridge University Press, New York, 2001.

Morgan, M.G. and D.W. Keith, Subjective judgements by climate experts, *Envirionmental Science and Technology, 29*, 468-476A, 1995.

Morita, T., J. Robinson, A. Adegbulugbe, J. Alcamo, D. Herbert, E. Lebre La Rovere, N. Nakicenovic, H. Pitcher, P. Raskin, K. Riahi, A. Sankovski, V. Sokolov, B. de Vries and D. Zhou, Greenhouse gas emission mitigation scenarios and implications, in *Climate Change 2001: Mitigation: Contribution of WGIII to the Third Assessment Report of the IPCC,* edited by B. Metz, O. Davidson, R. Swart and J. Pan, pp. 115-166, Cambridge University Press, New York, 2001.

Nakicenovic, N., J. Alcamo, G. Davis, B.d. Vries, J. Fenhann, S. Gaffin, K. Gregory, A. Grübler, T.Y. Jung, T. Kram, E.L.L. Rovere, L. Michaelis, S. Mori, T. Morita, W. Pepper, H. Pitcher, L. Price, K. Raihi, A. Roehrl, H.-H. Rogner, A. Sankovski, M. Schlesinger, P. Shukla, S. Smith, R. Swart, S.v. Rooijen, N. Victor and Z. Dadi, *IPCC Special Report on Emissions Scenarios,* Cambridge University Press, Cambridge, United Kingdom and New York, NY, USA, 2000.

Orr, J., E. Maier-Reimer, U. Mikolajewicz, P. Monfray, J.L. Sarmiento, J.R. Toggweiler, N.K. Taylor, J. Palmer, N. Gruber, C.L. Sabine, C. Le Quéré, R.M. Key and J. Boutin, Estimates of anthropogenic carbon uptake from four 3-D global ocean models, *Global Biogeochem. Cycles*, *15*, 43-60, 2001.

Orr, J.C. and J.-C. Dutay, OCMIP mid-project workshop, *Research GAIM Newsletter, 3*, 4-5, 1999.

Prentice, C., G. Farquhar, M. Fasham, M. Goulden, M. Heimann, V. Jaramillo, H. Kheshgi, C.L. Quéré, R. Scholes and D. Wallace, The carbon cycle and atmospheric CO_2, in *Climate Change 2001: The Scientific Basis: Contribution of WGI to the Third Assessment Report of the IPCC,* edited by J.T. Houghton et al., pp. In Press, Cambridge University Press, New York, 2001.

Ramaswamy, V., O. Boucher, J. Haigh, D. Hauglustaine, J. Haywood, G. Myhre, T. Nakajima, G.Y. Shi and S. Solomon, Radiative forcing of climate change, in *Climate Change 2001: The Scientific Basis: Contribution of WGI to the Third Assessment Report of the IPCC,* edited by J.T. Houghton et al., pp. 349-416, Cambridge University Press, New York, 2001.

Reilly, J., P.H. Stone, C.E. Forest, M.D. Webster, H.D. Jacoby and R.G. Prinn, Uncertainty and climate change assessments, *Science*, *293*, 430-433, 2001.

Sarmiento, J.L., T.M.C. Hughes, R.J. Stouffer and S. Manabe, Simulated response of the ocean carbon cycle to anthropogenic climate warming, *Nature, 393*, 245-249, 1998.

Sarmiento, J.L., U. Siegenthaler and J.C. Orr, A perturbation simulation of CO_2 uptake in an ocean general circulation model, *Journal of Geophysical Research, 97*, 3621-3645, 1992.

Schimel, D., D. Alves, I. Enting, M. Heimann, F. Joos, D. Raynaud and T. Wigley, CO_2 and the carbon cycle, in *Climate Change 1995: The Science of Climate Change: Contribution of WGI to the Second Assessment Report of the IPCC*, edited by J.T. Houghton et al., pp. 65-86, Cambridge University Press, New York, 1996.

Schimel, D., I. Enting, M. Heimann, T. Wigley, D. Raynaud, D. Alves and U. Siegenthaler, CO_2 and the carbon cycle, in *Climate Change 1994: Radiative Forcing of Climate Change and an Evaluation of the IPCC IS92 Emission Scenarios*, edited by J.T. Houghton et al., pp. 35-71, Cambridge University Press, New York, 1995.

Schneider, S.H., What is "dangerous" climate change?, *Nature, 411*, 17-19, 2001.

Schwartz, S.E. and M.O. Andreae, Uncertainty in climate change caused by aerosols, *Science, 272*, 1121-1122, 1996.

Siegenthaler, U. and F. Joos, Use of a simple model for studying oceanic tracer distributions and the global carbon cycle, *Tellus, 44B*, 186-207, 1992.

Sitch, S., *The role of vegetation dynamics in the control of atmospheric CO2 content* , Ph.D., University of Lund, Sweden, 2000.

Volk, T. and M.I. Hoffert, Ocean carbon pumps: Analysis of relative strengths and efficiencies in ocean-driven atmospheric CO_2 changes, in *Carbon Cycle and Atmospheric CO_2: Natural Variations Archean to Present*, edited by E. Sundquist and W.S. Broecker, pp. 91-110, Am. Geophys. Union, Washington, DC, 1985.

Watson, R.T., H. Rodhe, H. Oeschger and U. Siegenthaler, Greenhouse gases and aerosols, in *Climate Change, The IPCC Scientific Assessment*, edited by J.T. Houghton, G.J. Jenkins and J.J. Ephraums, pp. 1-40, Cambridge University Press, Cambridge, 1990.

Wigley, T.M.L., Balancing the carbon budget. Implications for projections of future carbon dioxide concentration changes, *Tellus, 45B*, 409-425, 1993.

Wigley, T.M.L., *The science of climate change: global and U.S. perspectives*, Pew Center on Global Climate Change, 1999.

Wigley, T.M.L., A.K. Jain, F. Joos, B.S. Nyenzi and P.R. Shukla, *Implications of Proposed CO_2 Emissions Limitations. IPCC Technical Paper 4*, Intergovernmental Panel on Climate Change, Bracknell, UK, 1997.

Wigley, T.M.L. and S.C.B. Raper, Interpretation of high projections for global-mean warming, *Science*, *293*, 451-454, 2001.

Wigley, T.M.L., R. Richels and J.A. Edmonds, Economic and environmental choices in the stabilization of CO_2 concentrations: choosing the "right" emissions pathway, *Nature*, *379*, 240-243, 1996.

Woodward, F.I., M.R. Lomas and R.A. Betts, Vegetation-climate feedbacks in a greenhouse world, *Philosophical Transactions of the Royal Society of London B*, *353*, 29-38, 1998.

Figure Captions

Fig. 1: Schematic diagram of the ISAM coupled atmosphere-ocean-biosphere model for the global carbon cycle.

Fig. 2: Scenario for atmospheric CO_2 concentration and average land temperature (excluding Antarctica) used in model intercomparisons.

Fig. 3: Ten year running mean of annual uptake from six dynamic global vegetation models (DGVMs) in response to a common scenario for atmospheric CO_2 concentration and climate: see in Fig. 2 [*Cramer et al.*, 2001].

Fig. 4: Comparison of modeled accumulation of carbon by plants, soils and detritus in response to (a) changes in atmospheric CO_2 concentration only, and (b) changes in atmospheric CO_2 concentration and climate (see Fig. 2). Accumulation counted starting in year 2000. Results of three parameterizations of ISAM (thick black curves) calibrated to match the average (of the LPJ, IBIS and SDGVM) and range of the six DGVMs.

Fig. 5: Comparison of modeled (a) annual uptake, and (b) accumulation of carbon in the oceans in response to changes in atmospheric CO_2 concentration following the CO_2 scenario shown in Fig. 2. Accumulation counted starting in year 2000. Results of three parameterizations of ISAM (thick black curves) calibrated to match the average and range of the 10 coupled ocean/atmosphere models.

Fig. 6: Observation-based estimates of global temperature anomaly and atmospheric CO_2 specified as inputs for ISAM over the period from 1765 to 1999 for reconstruction of past carbon cycle and computation of initial conditions for future projections.

Fig. 7: Projections of CO_2 concentration and global average near-surface temperature driven by the benchmark emission scenario IS92a [*Leggett et al.*, 1992]. This future non-intervention emission scenario for CO_2 emissions from fossil fuels and cement production is shown in (a). Specifying this scenario, the solid curves show the ISAM projections (using the reference parameterization) of CO_2 concentrations in (b) and global temperatures in (c). Temperature is given as an anomaly from mid-1800s (see Section 4.3 and Fig. 6). The highest and lowest projections (high and low parameterizations of ISAM) are shown by the dashed curves. Projected CO_2 concentrations are also shown by the labeled curves when the climate/carbon cycle interaction is not included (for reference ISAM parameters) and as reported in the IPCC Second Assessment Report [*Schimel et al.*, 1996]. Observation-based estimates are shown by the circles prior to 2000.

Fig. 8: Projections of CO_2 concentration and global average near-surface temperature driven by the IPCC SRES [*Nakicenovic et al.*, 2000] emission scenarios. The 6 illustrative scenarios of CO_2 emissions from fossil fuels and cement production are shown in (a). Projections of (b) CO_2 concentrations and (c) global temperatures for the 6 scenarios are shown by the plotted symbols for the reference parameterization of ISAM. Temperature is given as an anomaly from mid-1800s (see Section 4.3 and Fig. 6). The highest and lowest projections (high and low parameterizations of ISAM) are shown by the shaded area for only

scenario A1B, and for all 6 scenarios by the dashed curves. Observation-based estimates are shown by the circles prior to 2000.

Fig. 9: Projections of CO_2 emissions and global average near-surface temperature driven by specified concentrations pathways (a) leading to constant CO_2 concentrations ranging from 450 to 1000 ppm specified by Wigley et al. [1996]. Estimates of (b) *anthropogenic* (i.e., fossil plus land use) CO_2 emissions, and (c) global average near-surface temperature anomaly deduced from specified concentrations pathways are shown by the solid curves for the reference parameterization of ISAM. Temperature is given as an anomaly from mid-1800s (see Section 4.3 and Fig. 6). The highest and lowest projections (low and high parameterizations of ISAM for emissions, and high and low parameterizations for temperature) are shown by the shaded area for only the pathway leading to stabilizaiton at 550 ppm, and for all 5 pathways by the dashed curves. Prior to 2000, observation-based estimates of (a) CO_2 concentrations, (b) <u>fossil</u> CO_2 emissions, and (c) temperature anomaly are shown by the circles.

Table 1. Model-based reconstructions of past carbon budgets.

	Budget Period											
	1980 - 1989			**1990 - 1999**			**1850 - 1989**			**1765 - 1999**		
Observation-based Quantities, GtC												
a) Fossil CO_2 emissions	**54.5**			**63.3**			**212.0**			**276.5**		
b) Atmospheric CO_2 accumulation	**33.3**			**32.9**			**137.1**			**189.0**		
Model-based Quantities, GtC												
Model parameterization ⇒	**ref**	**low**	**high**	**ref**	**low**	**high**	**ref**	**low**	**high**	**ref**	**low**	**high**
c) Ocean sink	**16.5**	18.2	14.4	**18.6**	20.6	16.0	**93.7**	104.6	80.1	**125.2**	139.2	107.8
d) Net terrestrial sink (= a - b - c)	**4.6**	2.9	6.8	**11.8**	9.7	14.4	**-18.9**	-29.8	-5.2	**-37.7**	-51.6	-20.3
e) Terrestrial sink in response to climate and CO_2 change	**13.3**	22.8	9.2	**15.0**	25.0	10.8	**77.5**	133.2	54.1	**103.5**	178.2	71.9
f) Land use source (= e - d)	**8.7**	19.9	2.4	**3.2**	15.2	-3.6	**96.3**	163.0	81.8	**141.2**	229.9	92.2

Table 2. Carbon budgets for the 21st century for IPCC emission scenarios.

	Change in Carbon Stocks from 2000 to 2099, GtC†										
	Fossil Fuels‡	Land Use	Plants & Soils*			Oceans			Atmosphere		
Model parameterization⇒			ref	low	high	ref	low	high	ref	low	high
IPCC Scenario											
IS92a	-1360.4	-68.2	236.5	401.6	130.7	379.6	389.2	317.3	744.2	569.5	912.4
A1B	-1363.6	-50.3	242.2	412.4	150.3	385.1	397.8	324.2	736.3	553.5	889.1
A1T	-968.5	-19.4	200.1	330.6	126.2	312.9	321.2	261.0	455.5	316.7	581.3
A1FI	-2046.2	-50.9	313.8	537.5	199.2	469.6	495.6	392.4	1262.8	1013.2	1454.6
A2	-1695.9	-77.5	253.4	445.9	153.6	422.8	441.0	356.1	1019.7	809.1	1186.2
B1	-919.4	16.8	236.0	355.5	167.5	297.8	302.5	252.0	385.6	261.3	499.9
B2	-1086.0	7.4	238.6	371.7	165.3	314.5	322.9	264.5	532.9	391.5	656.3

† **Budget period extends from the start of 2000 to the end of 2099. This leads to a slight discrepancy with the cumulative emissions reported in the IPCC Special Report on Emission Scenarios that apparently accumulates emissions from mid-year to mid-year, provided the reported emissions are per annum as is consistent with the initial (1990) emissions data.**

* **The change in plant and soil carbon stocks includes that due to land use change, an equivalent definition to row e in Table 1.**

Table 3. Carbon budgets over the next three centuries for CO_2 stabilization.

Budget Period	Stabilization Level, ppm	Carbon Stock Change over Budget Period, GtC				
		Atm.		Ocean	Plants and Soils**	Fossil**
2000-2099	**450**	**176.2**	ref.	222.0	86.8	-485.0
			low	274.5	230.9	-681.7
			high	157.0	18.5	-351.7
	550	**367.6**	ref.	297.7	154.7	-820.0
			low	360.1	350.4	-1078.2
			high	220.7	63.8	-652.2
	650	**497.1**	ref.	334.9	188.8	-1020.8
			low	401.5	409.7	-1308.3
			high	252.7	87.2	-837.1
	750	**573.2**	ref.	353.1	205.8	-1132.2
			low	421.8	438.9	-1433.9
			high	268.7	99.0	-940.9
	1000	**650.4**	ref.	368.5	220.2	-1239.1
			low	438.5	463.3	-1552.3
			high	264.8	126.6	-1041.9
2100-2199	**450**	**0.0**	ref.	130.4	29.2	-159.6
			low	183.1	73.5	-256.6
			high	67.1	-0.5	-66.6
	550	**20.8**	ref.	202.6	62.4	-285.8
			low	276.5	144.1	-441.4
			high	113.4	11.5	-145.7
	650	**103.6**	ref.	269.2	104.8	-477.6
			low	358.5	226.4	-688.6
			high	161.3	33.2	-298.0
	750	**225.8**	ref.	321.5	143.3	-690.5
			low	421.1	298.0	-944.9
			high	201.2	55.1	-482.1
	1000	**504.0**	ref.	397.5	205.3	-1106.8
			low	509.9	409.9	-1423.8
			high	158.3	-0.4	-662.0
2200-2299	**450**	**0.0**	ref.	101.4	13.5	-114.9
			low	150.0	36.6	-186.6
			high	44.4	-3.3	-41.1
	550	**0.0**	ref.	148.5	20.5	-169.0
			low	217.3	56.9	-274.3
			high	67.7	-5.8	-61.9
	650	**0.0**	ref.	189.8	28.1	-217.9
			low	274.8	78.9	-353.8
			high	89.6	-8.0	-81.6
	750	**14.0**	ref.	229.5	40.7	-284.2
			low	327.9	109.2	-451.1
			high	113.4	-6.6	-120.8
	1000	**167.8**	ref.	313.2	82.7	-563.7
			low	433.7	196.8	-798.3
			high	170.7	9.4	-347.9

* Deduced decrease in fossil stocks equals net increase in atmosphere, ocean, and plant and soil stocks

** Plant and soil stock change includes contribution from changing land use of -68.2 GtC over 2000-2099, and zero over the later periods.

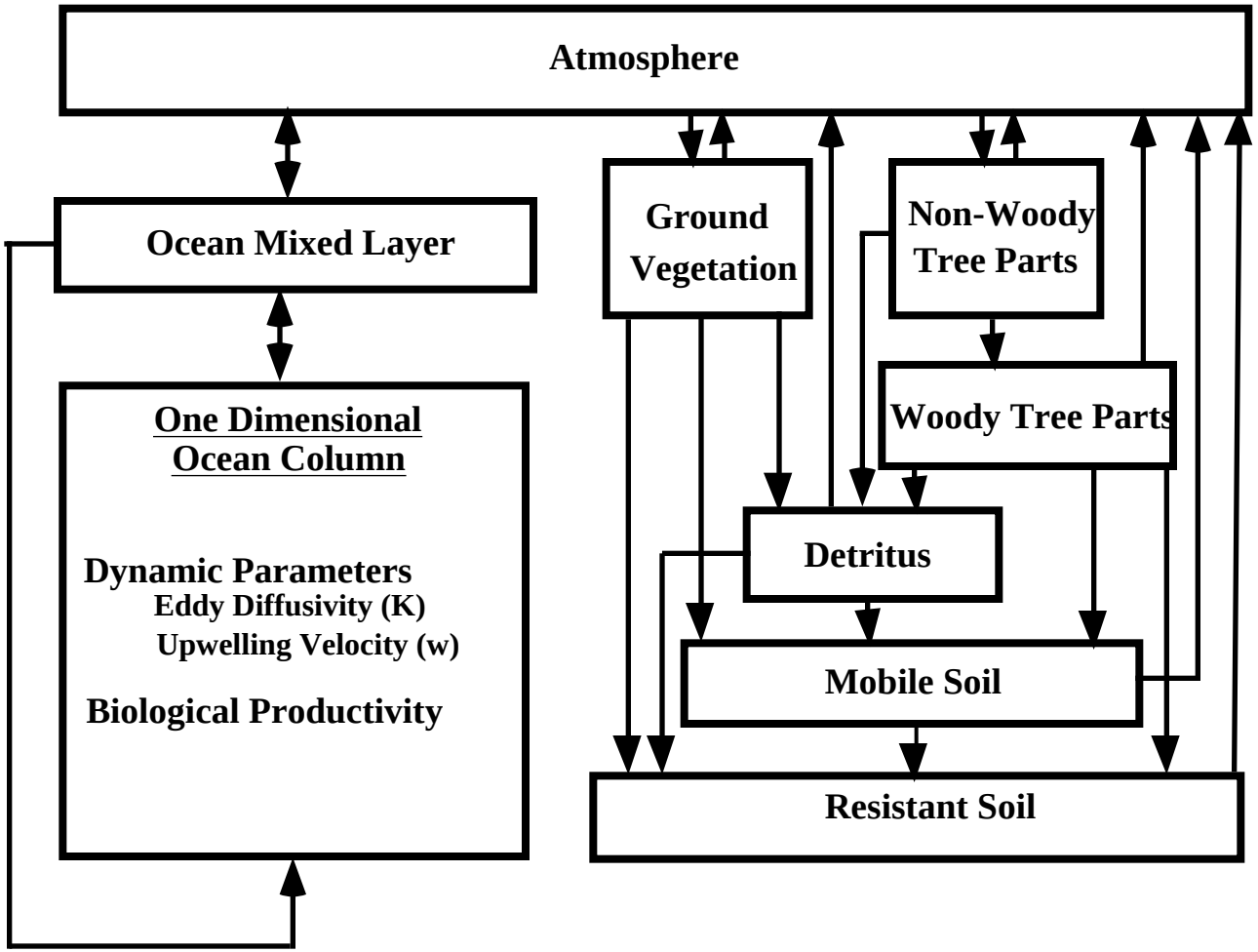
Atmosphere
Ocean Mixed Layer
One Dimensional
Ocean Column
Dynamic Parameters
Eddy Diffusivity (K)
Upwelling Velocity (w)
Biological Productivity
Ground
Vegetation
Non-Woody
Tree Parts
Woody Tree Parts
Detritus
Mobile Soil
Resistant Soil

Figure 1

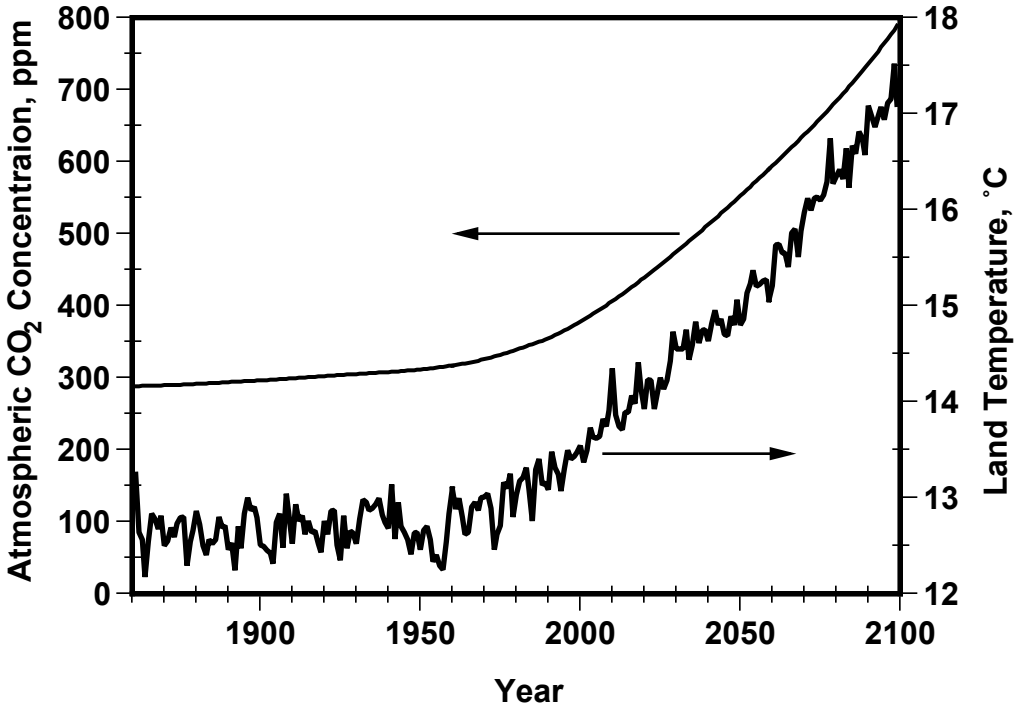
Atmospheric CO_2 Concentraion, ppm
Land Temperature, ˚C
Year
800
700
600
500
400
300
200
100
0
18
17
16
15
14
13
12
1900
1950
2000
2050
2100

Figure 2

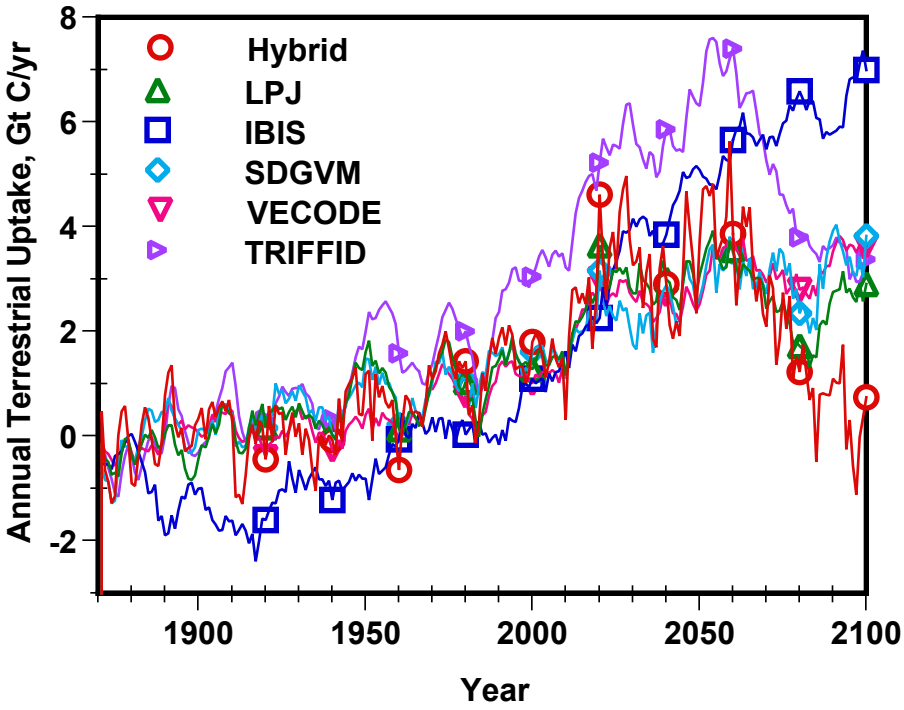
Annual Terrestrial Uptake, Gt C/yr
8
6
4
2
0
-2
1900
1950
2000
2050
2100
Year
Hybrid
LPJ
IBIS
SDGVM
VECODE
TRIFFID

Figure 3

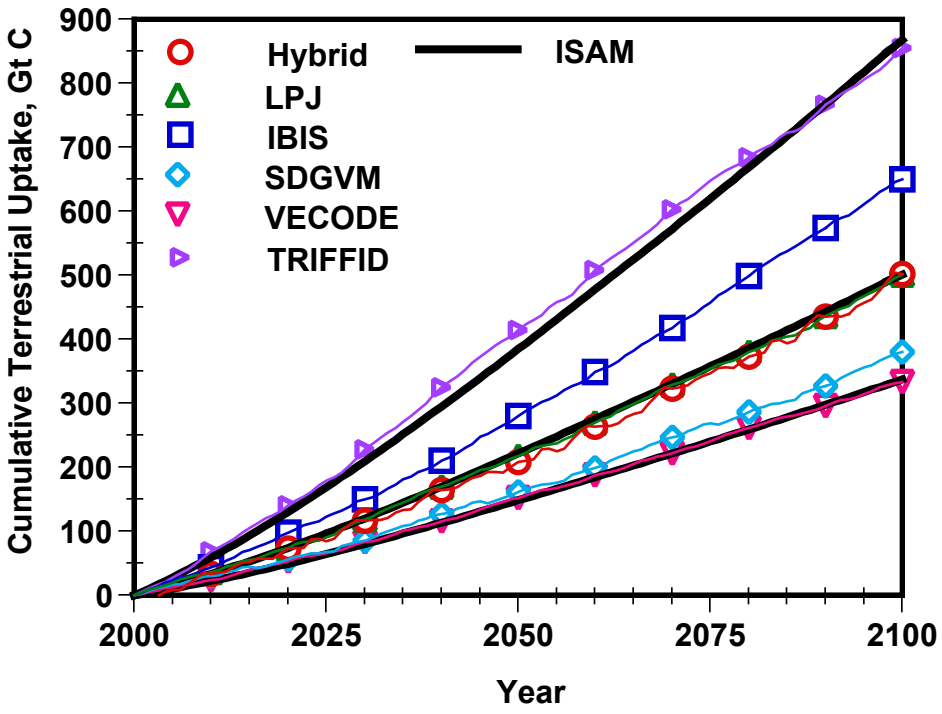
Cumulative Terrestrial Uptake, Gt C
900
800
700
600
500
400
300
200
100
0
2000
2025
2050
2075
2100
Year
Hybrid
ISAM
LPJ
IBIS
SDGVM
VECODE
TRIFFID

Figure 4a

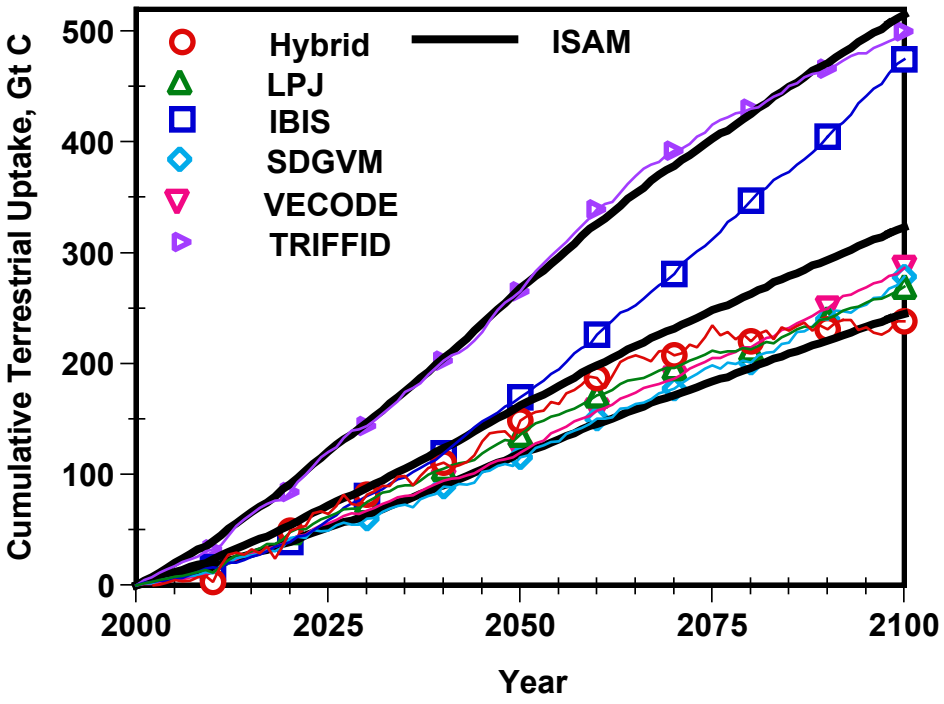
Cumulative Terrestrial Uptake, Gt C
500
400
300
200
100
0
2000
2025
2050
2075
2100
Year
Hybrid
ISAM
LPJ
IBIS
SDGVM
VECODE
TRIFFID

Figure 4b

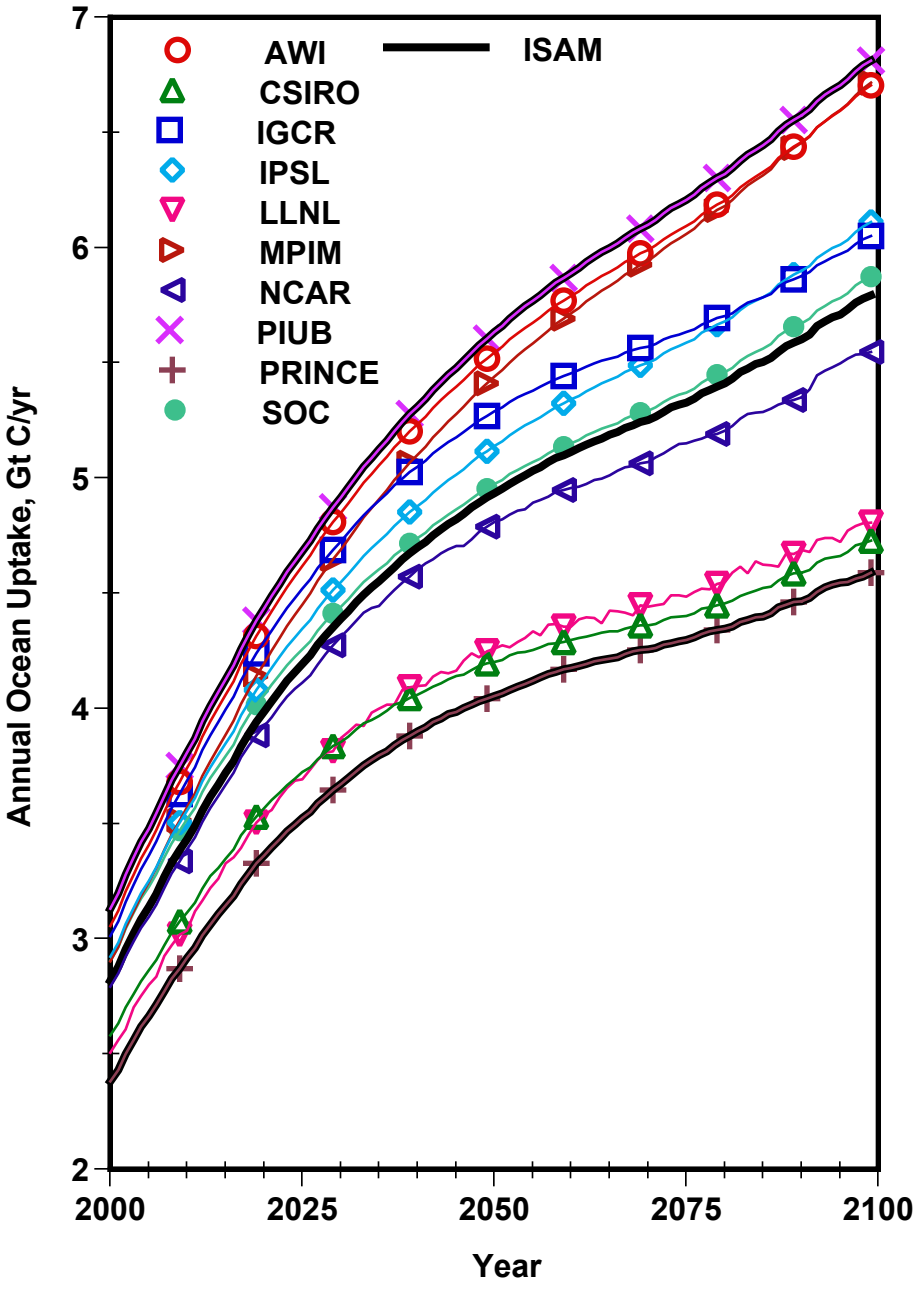
AWI
CSIRO
IGCR
IPSL
LLNL
MPIM
NCAR
PIUB
PRINCE
SOC
ISAM
Annual Ocean Uptake, Gt C/yr
Year
2
3
4
5
6
7
2000
2025
2050
2075
2100

Figure 5a

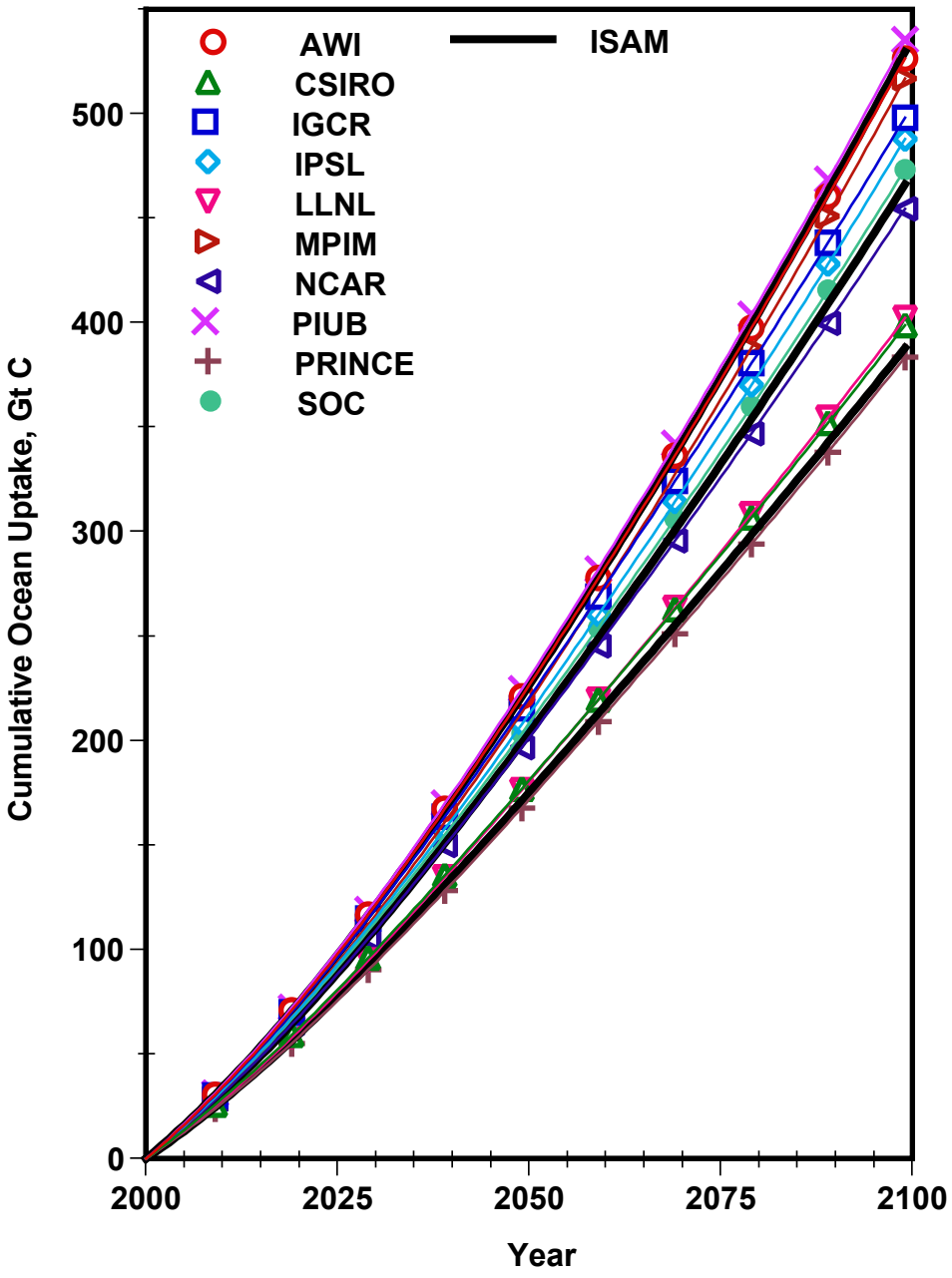
AWI
CSIRO
IGCR
IPSL
LLNL
MPIM
NCAR
PIUB
PRINCE
SOC
ISAM
Cumulative Ocean Uptake, Gt C
0
100
200
300
400
500
2000
2025
2050
2075
2100
Year

Figure 5b

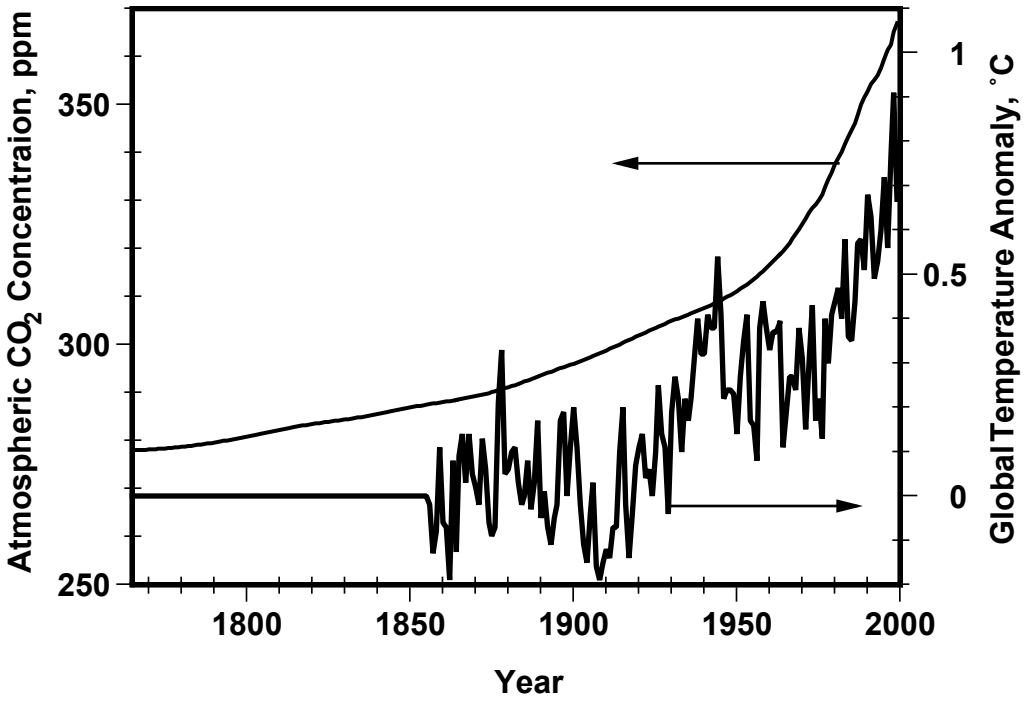
Atmospheric CO_2 Concentraion, ppm
350
300
250
1800
1850
1900
1950
2000
Year
1
0.5
0
Global Temperature Anomaly, ˚C

Figure 6

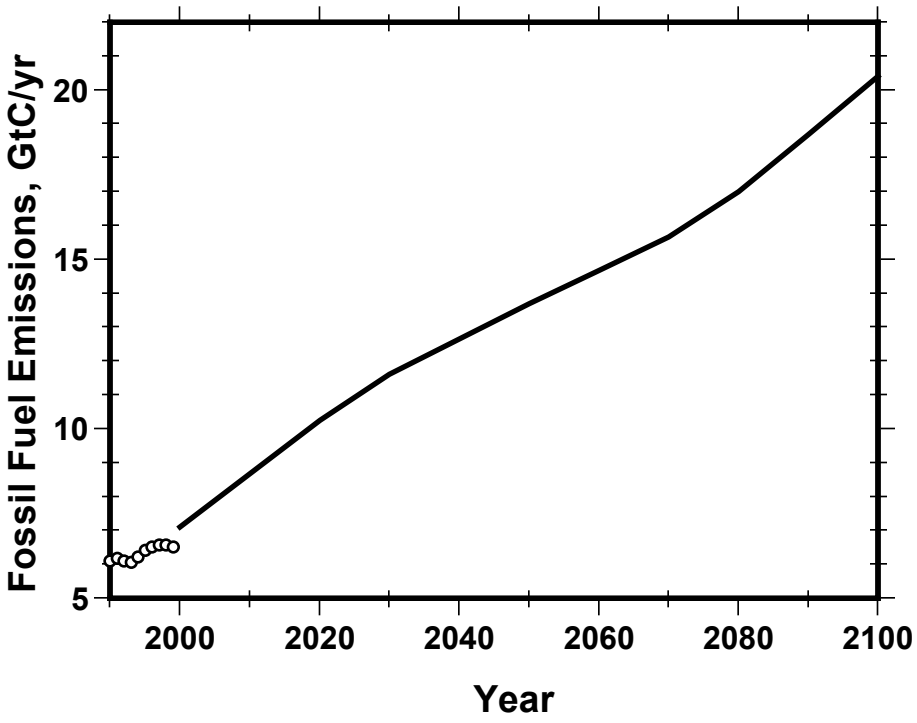
Fossil Fuel Emissions, GtC/yr
20
15
10
5
2000
2020
2040
2060
2080
2100
Year

Figure 7a

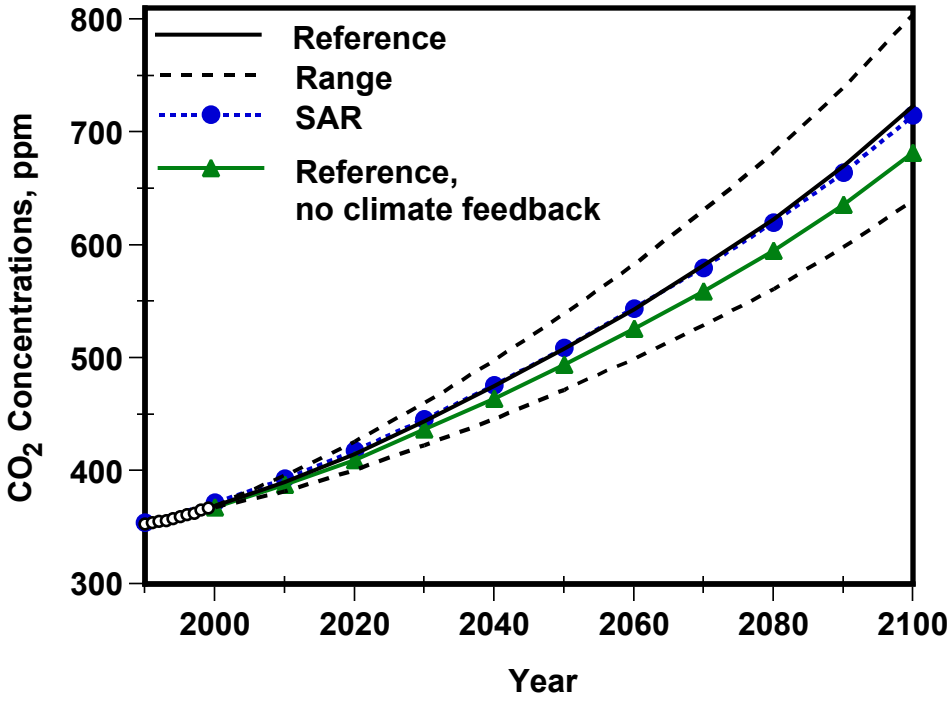
800
700
600
500
400
300
CO_2 Concentrations, ppm
2000
2020
2040
2060
2080
2100
Year
Reference
Range
SAR
Reference,
no climate feedback

Figure 7b

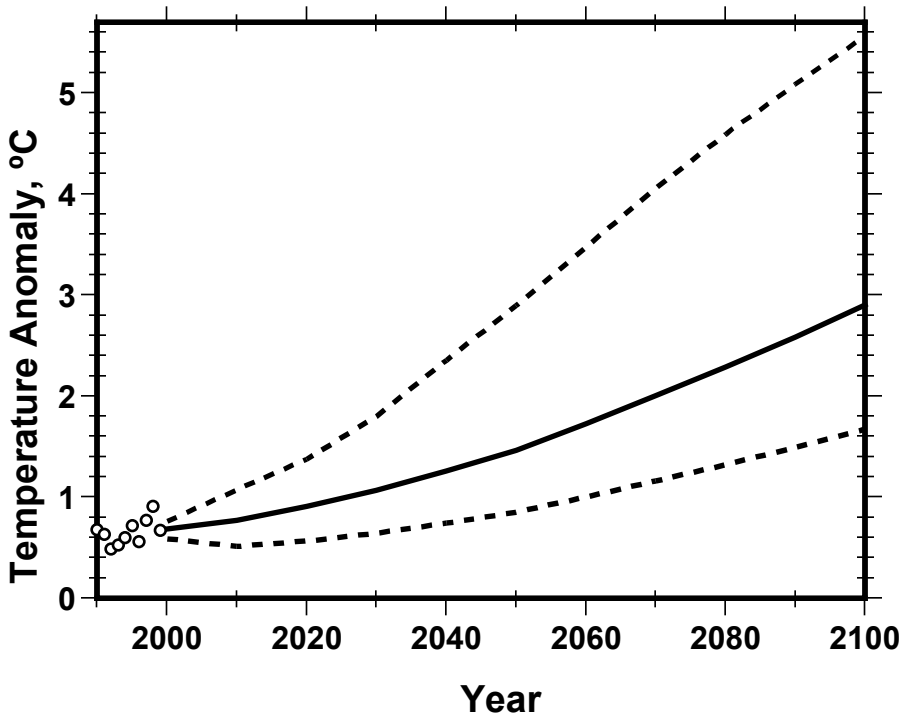
Temperature Anomaly, °C
0
1
2
3
4
5
2000
2020
2040
2060
2080
2100
Year

Figure 7c

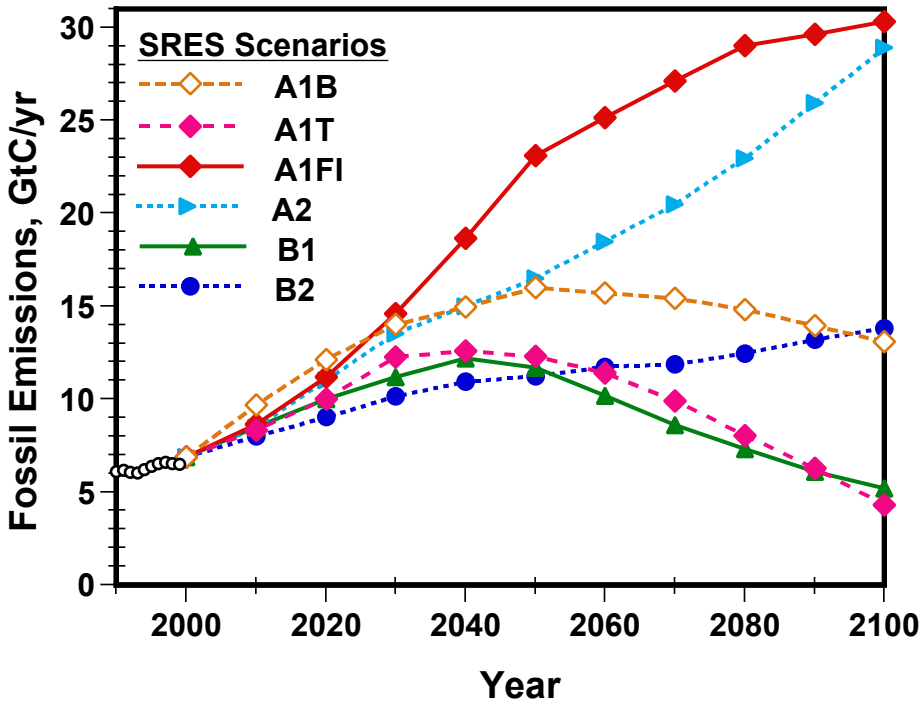
SRES Scenarios
A1B
A1T
A1FI
A2
B1
B2
Fossil Emissions, GtC/yr
0
5
10
15
20
25
30
2000
2020
2040
2060
2080
2100
Year

Figure 8a

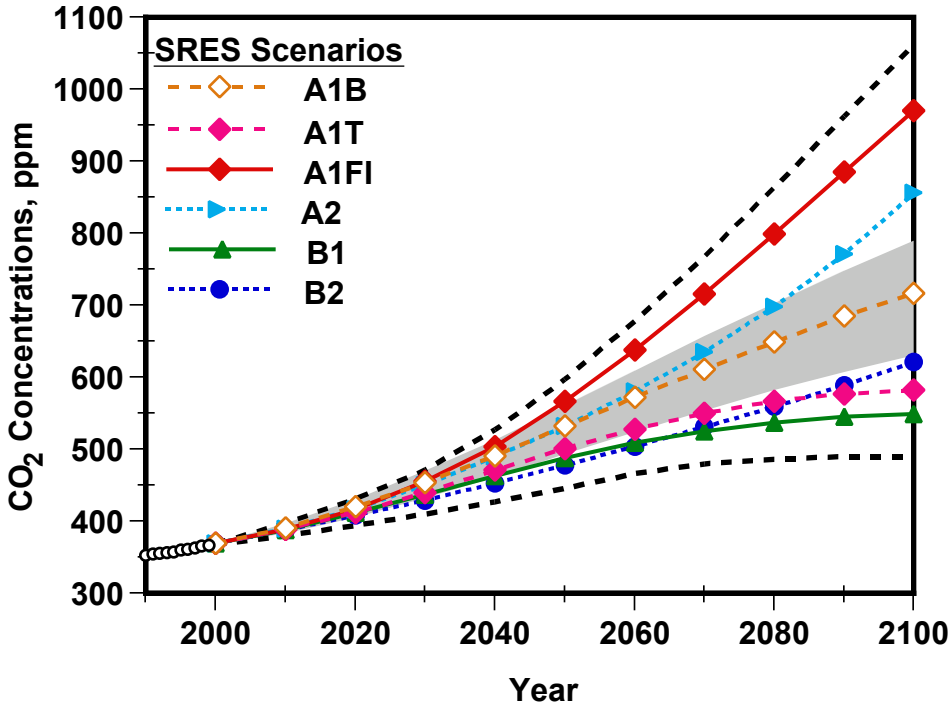
SRES Scenarios
A1B
A1T
A1FI
A2
B1
B2
CO_2 Concentrations, ppm
1100
1000
900
800
700
600
500
400
300
2000
2020
2040
2060
2080
2100
Year

Figure 8b

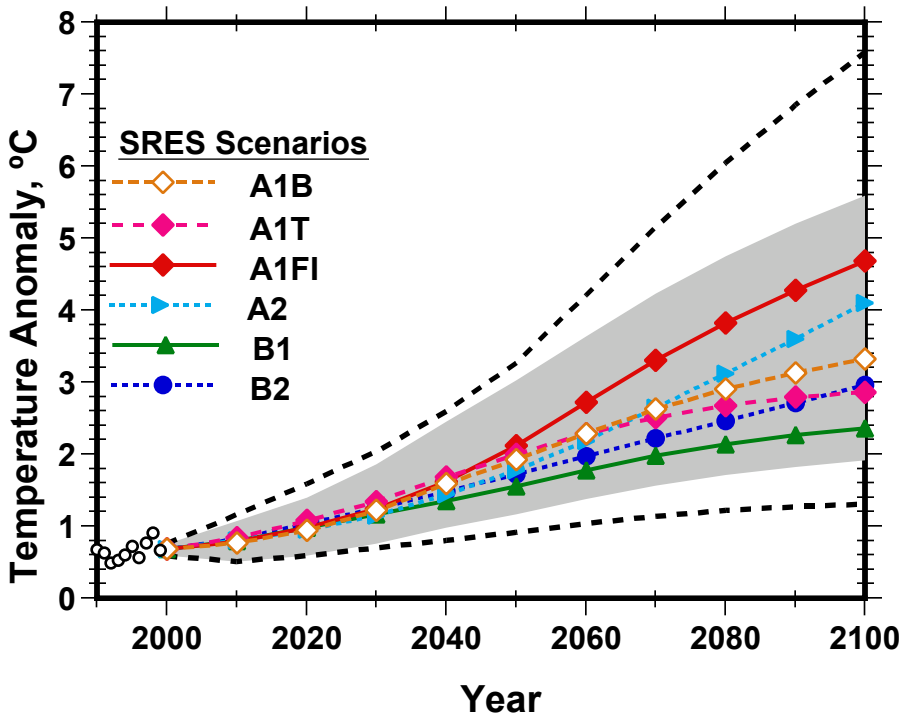
SRES Scenarios
A1B
A1T
A1FI
A2
B1
B2
Temperature Anomaly, °C
Year
0
1
2
3
4
5
6
7
8
2000
2020
2040
2060
2080
2100

Figure 8c

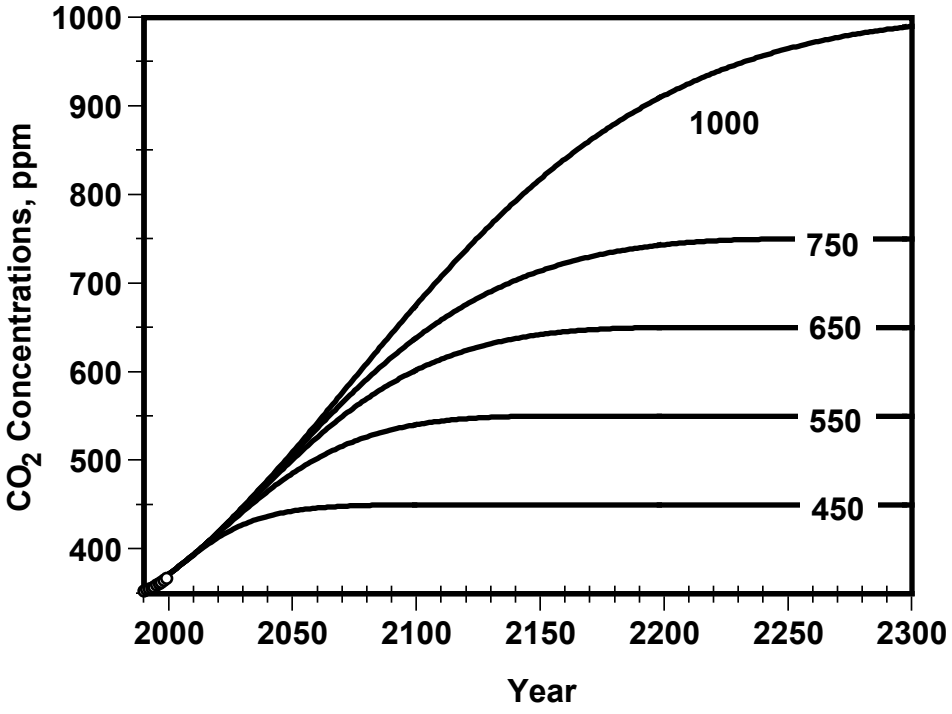
1000
900
800
700
600
500
400
CO_2 Concentrations, ppm
1000
750
650
550
450
2000
2050
2100
2150
2200
2250
2300
Year

Figure 9a

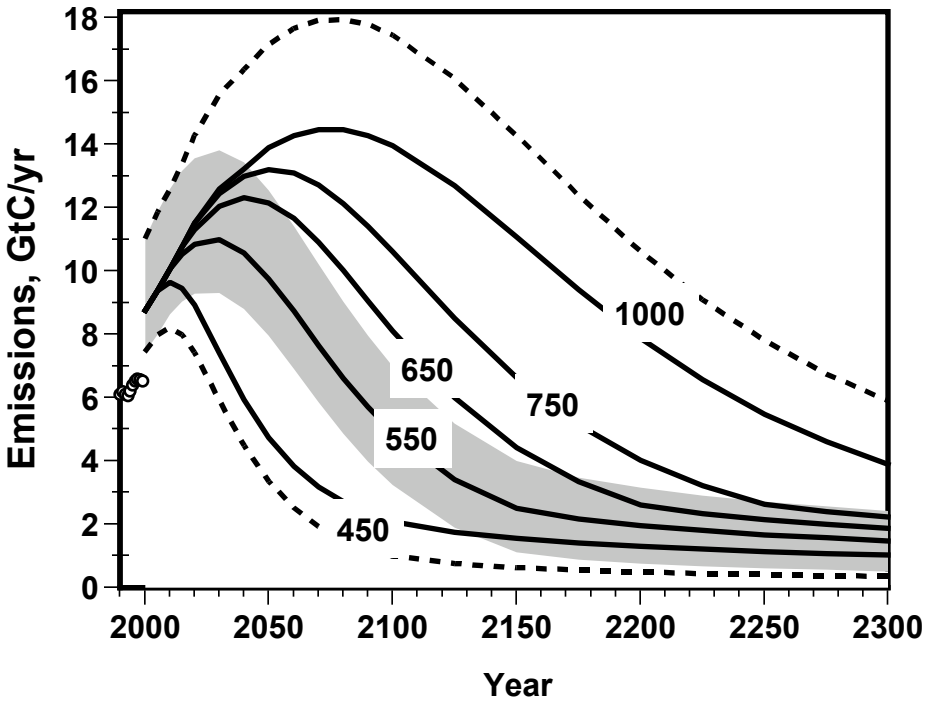
Emissions, GtC/yr
Year
18
16
14
12
10
8
6
4
2
0
2000
2050
2100
2150
2200
2250
2300
1000
750
650
550
450

Figure 9b

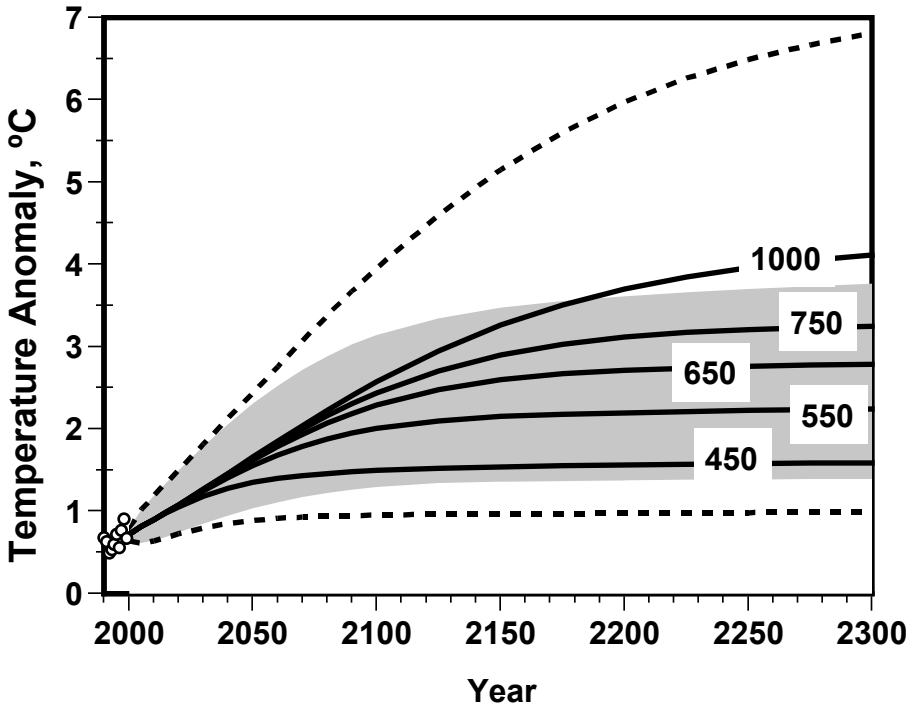
Temperature Anomaly, °C
Year
0
1
2
3
4
5
6
7
2000
2050
2100
2150
2200
2250
2300
1000
750
650
550
450

Figure 9c